TERRAIN PROFILING FROM SEASAT ALTIMETRY

R. L. Brooks

GeoScience Research Corporation
Route 4 Box 129
Salisbury, Maryland 21801

MAY 1981

FOREWORD

This Seasat altimeter overland study was jointly funded by the National Geodetic Survey and the U. S. Geological Survey.

GeoScience Research Corporation appreciates the valuable technical guidance provided by the following individuals:

Bernard Chovitz, National Geodetic Survey
Patricia Gaborski, National Geodetic Survey
William Schoonmaker, U. S. Geological Survey
Lee Bender, U. S. Geological Survey
Doug Carter, U. S. Geological Survey.
William Krabill, National Aeronautics and Space Administration

TABLE OF CONTENTS

INTRODUCTION

Seasat radar altimeter overland measurements have been analyzed over selected geographic areas to determine their applicability for terrain profiling. Even though the expected Seasat useful life was shortened considerably, the altimeter overland data base consists of over 400 hours at a measurement rate of 0.1 second. Considering the Seasat groundtrack velocity of 7 km sec^{-1}, the data base represents potential overland profiling lengths of approximately 1 X 10^7km. Even if only 10% of the overland data is geodetically useful, or can be made useful, this represents a very significant data base for terrain mapping, regional tectonic studies, monitoring of vertical crustal movements, and ice sheet topography.

ALTIMETER DATA PROCESSING

A surface elevation corresponding to each altimeter height measurement may be computed by algebraically subtracking the measured height (A) from the computed satellite height based on orbital computations (H). This surface height is with respect to the Seasat orbit reference ellipsoid and, in order to achieve surface heights referenced to Mean Sea Level (E), the geoid-ellipsoid separations (G) must be subtracted as

$$E = H - A - G \quad (1)$$

where all units are in meters.

The orbital computations generally provide H accurate to within a few meters. The error in H has a long wavelength and is considered constant for each geographic area involved in this analysis. To compensate for the orbit-to-orbit differences in H, each Seasat pass was zero-set on flat terrain or a water surface with known elevation.

The processing utilized the GEM-8 geoid model. No smoothing or filtering was applied to the altimeter measurements.

RESULTS

The Seasat altimeter overland analyses are summarized for the following geographic areas:

1) Andean salars of southern Bolivia
2) Alaska
3) south-central Arizona
4) Imperial Valley of California
5) Yuma Valley of Arizona
6) Great Salt Lake Desert

Analysis of the data over all of these geographic areas has shown that the Seasat altimeter tracking servo did not respond quickly enough to changing terrain features. However, it is demonstrated that retracking of the archived surface return waveforms yields surface elevations over smooth terrain accurate to ± 1 m when correlated with large-scale maps.

The following discussion will initially describe the retracking algorithm and its verification over the Andean salars of southern Bolivia. The results for each of the six geographic areas will then be presented.

WAVEFORM RETRACKING

The objective of the Seasat waveform retracking is to reposition the tracking gate with respect to the sampled waveforms. Over the open ocean, the goal of the altimeter designers was to position the tracking gate on the leading edge of the waveform at the point corresponding to 50% of the peak power in the waveform. Due to dynamic height changes of the open-ocean being very small, the altimeter tracking design served its purpose and maintained tracking very well at the 50% point. The onboard height processor was optimized also for an expected non-specular return from ocean surface.

Once over land, however, the tracker encountered both specular returns and larger dynamic height rates. This usually resulted in mispositioning of the tracking gate; fortunately, the sampled waveforms were preserved in the data base and may be retracked.

The Seasat tracker had 60 waveform sampling gates with a separation of 3.125 ns or, equivalently, 46.84 cm. These gates are arbitrarily numbered from -30 (early gate) to +30 (late gate) with the desired tracking point at the mid-point between the -1 and +1 gates (0^{th} gate). The corrected surface elevation, E_c, is computed as

$$E_c = E - 0.4684\, g \quad (2)$$

where g is the interpolated gate number corresponding to the 50% level of the sampled peak power per waveform. The waveforms were telemetered to the ground at a rate of 10 per second, the same rate as the range measurements. Each of the recorded waveforms is the average of two consecutive waveforms sampled at a rate of 20 per second.

During the search for a suitable area to evaluate retracking algorithms, the salars (salt-encrusted playas) in the high Andes of southern Bolivia were brought to our attention by W. D. Carter of the U. S. Geological Survey. Stoertz and Carter (1976) had analyzed Landsat imagery of this area for hydrologic and geologic data. Due to the lack of man-made structures and lack of vegetation, the salars are well suited to being evaluation areas for the Seasat altimeter retracking algorithms.

A search was made of the Seasat altimeter data base to find altimeter passes over the two largest salars, Salar de Uyuni and Salar de Coipasa. These two salars and the altimeter geometry traversing them are shown in Figure 1. Particular emphasis has been placed on the Salar de Uyuni; it is at an altitude of about 3653 meters and covers an area of almost 10,000 km^2, which makes it the largest flat, salt-covered surface on earth (Carter, et al, in press). During the rainy Bolivian winter, the Salar de Uyuni becomes flooded by runoff from the nearby mountains. During most of the year, however, the surface is relatively dry and hard.

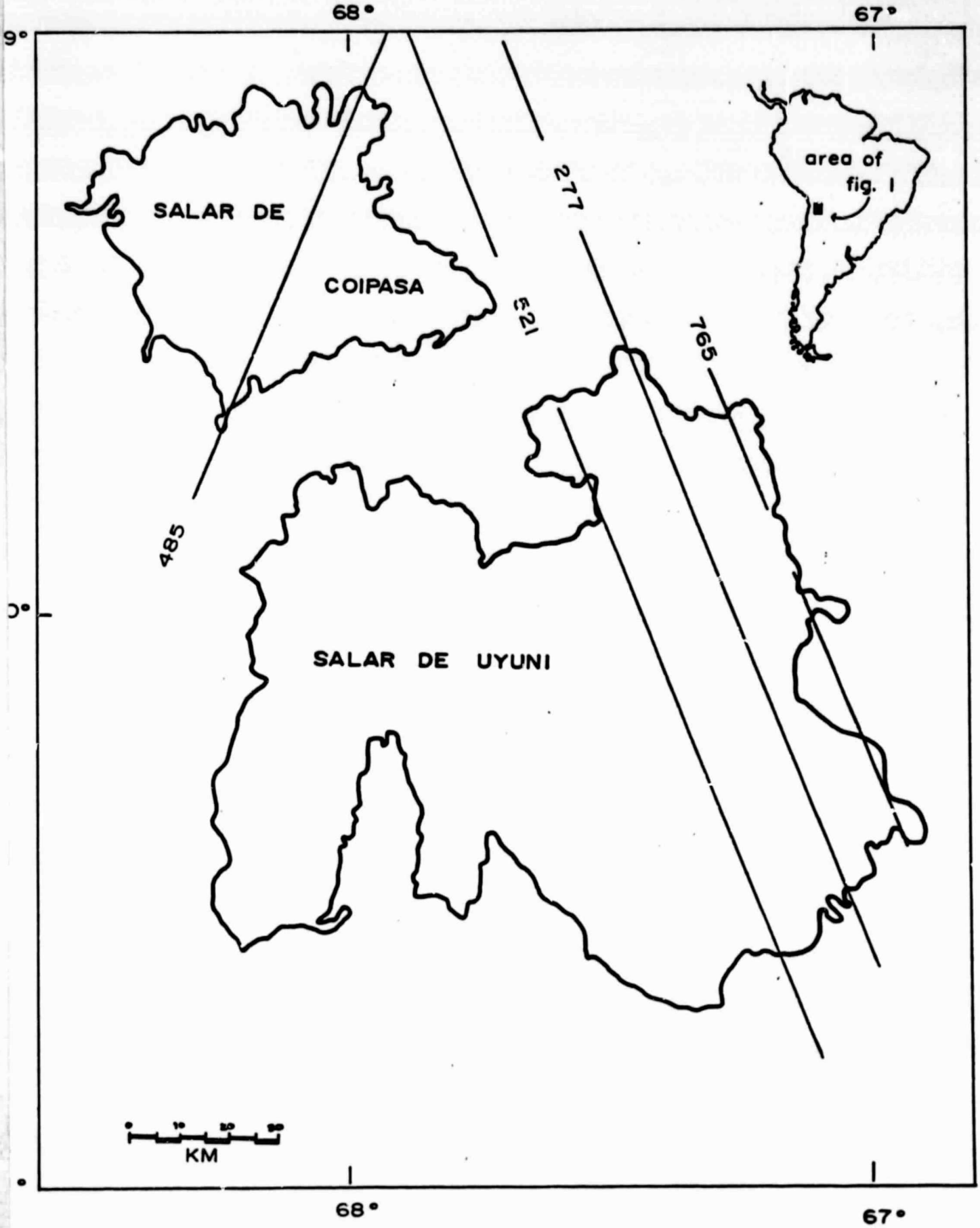

Figure 1 - Seasat Altimeter Groundtracks over Salar de Uyuni and Salar de Coipasa.

An interesting sidelight of this altimeter retracking over the relatively unexplored Salar de Uyuni is that valuable potassium and lithium salts are found to accumulate in brine pockets (Carter, el al, in press). This altimeter retracking and resultant profiling could perhaps locate areas of slightly lower elevations where surface ponding would persist longer than in other areas, producing higher concentrations of these salts.

A typical specular Seasat waveform over the Salar de Uyuni is in Figure 2 where, prior to retracking, the 50% peak power point is at the interpolated gate value of +0.60. Following equation (2), the computed surface elevation for this sample would decrease by 0.281 m as the result of retracking.

To illustrate waveform movement near the tracking gate, eight consecutive waveforms over Salar de Uyuni from orbit 277 are shown in Figure 3.

The improvement in the surface elevations as the result of retracking 16 consecutive waveforms sets across 10 km of the salt flat is shown at a greatly expanded vertical scale in Figure 4. Comparison of surface elevations before and after retracking is extended to a distance of 125 km in Figure 5 where the first 30 km is the salar shoreline on the south-eastern rim.

Examination of the retracked profile in Figure 5 shows that a few data spikes remain; correlation of the data spikes with waveforms shows that each data spike over the Salar de

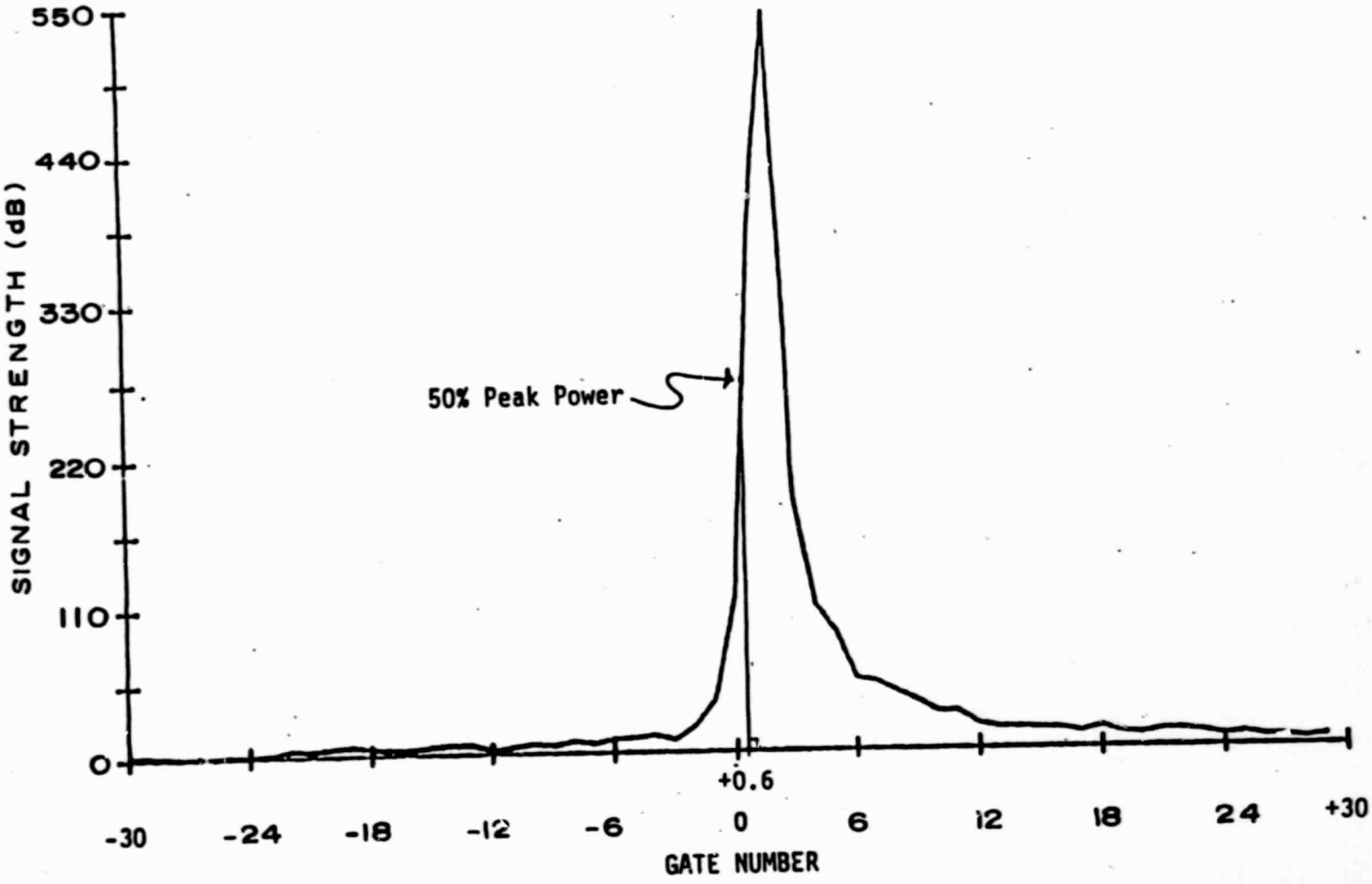

Figure 2 - Typical Altimeter Waveform from Salar de Uyuni Surface Illustrating Rapid Rise-Time and Rapid Decay of Waveform. Also Illustrated is a 0.6 Gate Mispositioning of the Seasat Tracking Point.

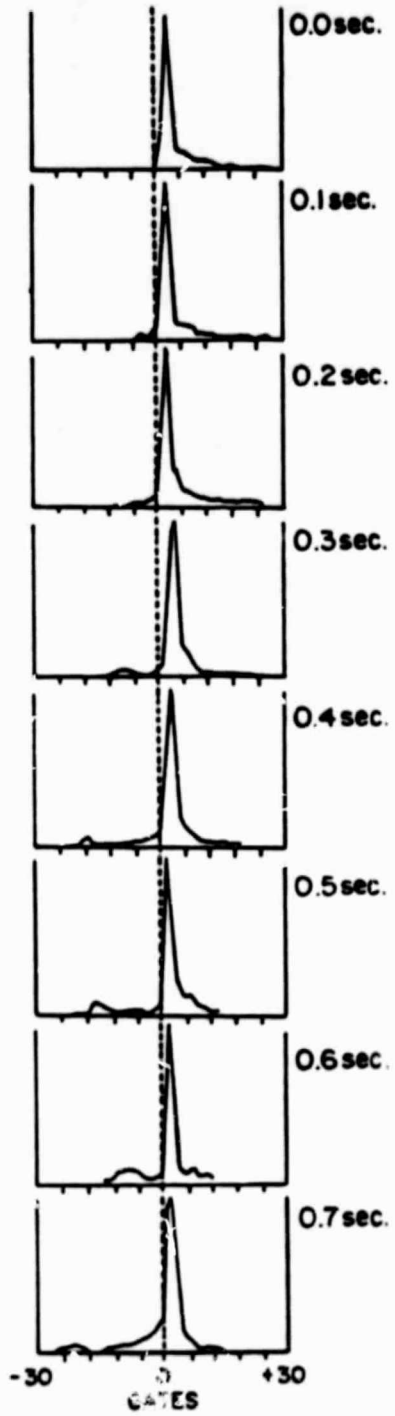

Figure 3 - Eight Consecutive Altimeter Waveforms over Salar de Uyuni, Illustrating Movement of Waveforms with Respect to the 0^{th} (Tracking) Gate. Each Gate Width is Equivalent to 46.84 cm.

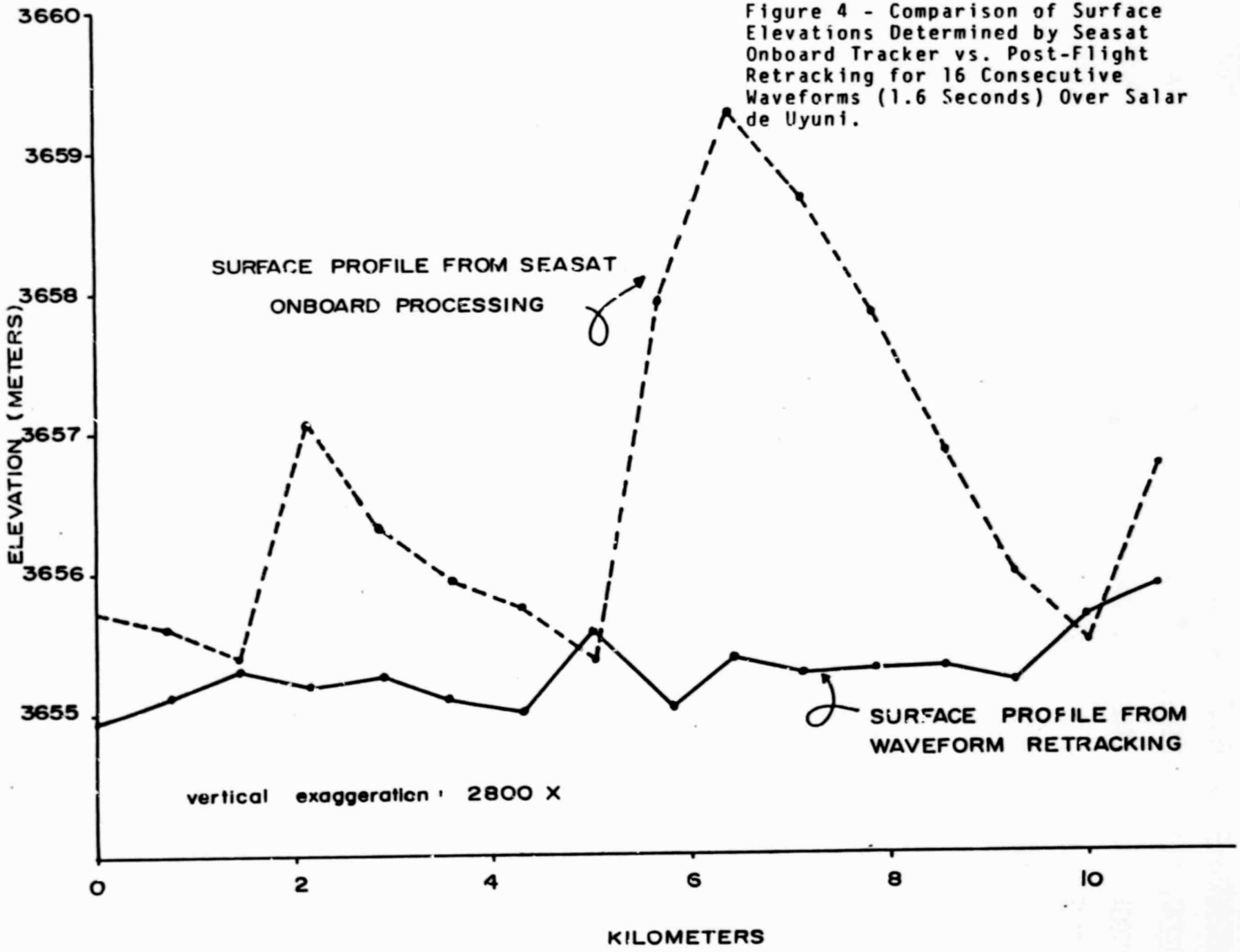

Figure 4 - Comparison of Surface Elevations Determined by Seasat Onboard Tracker vs. Post-Flight Retracking for 16 Consecutive Waveforms (1.6 Seconds) Over Salar de Uyuni.

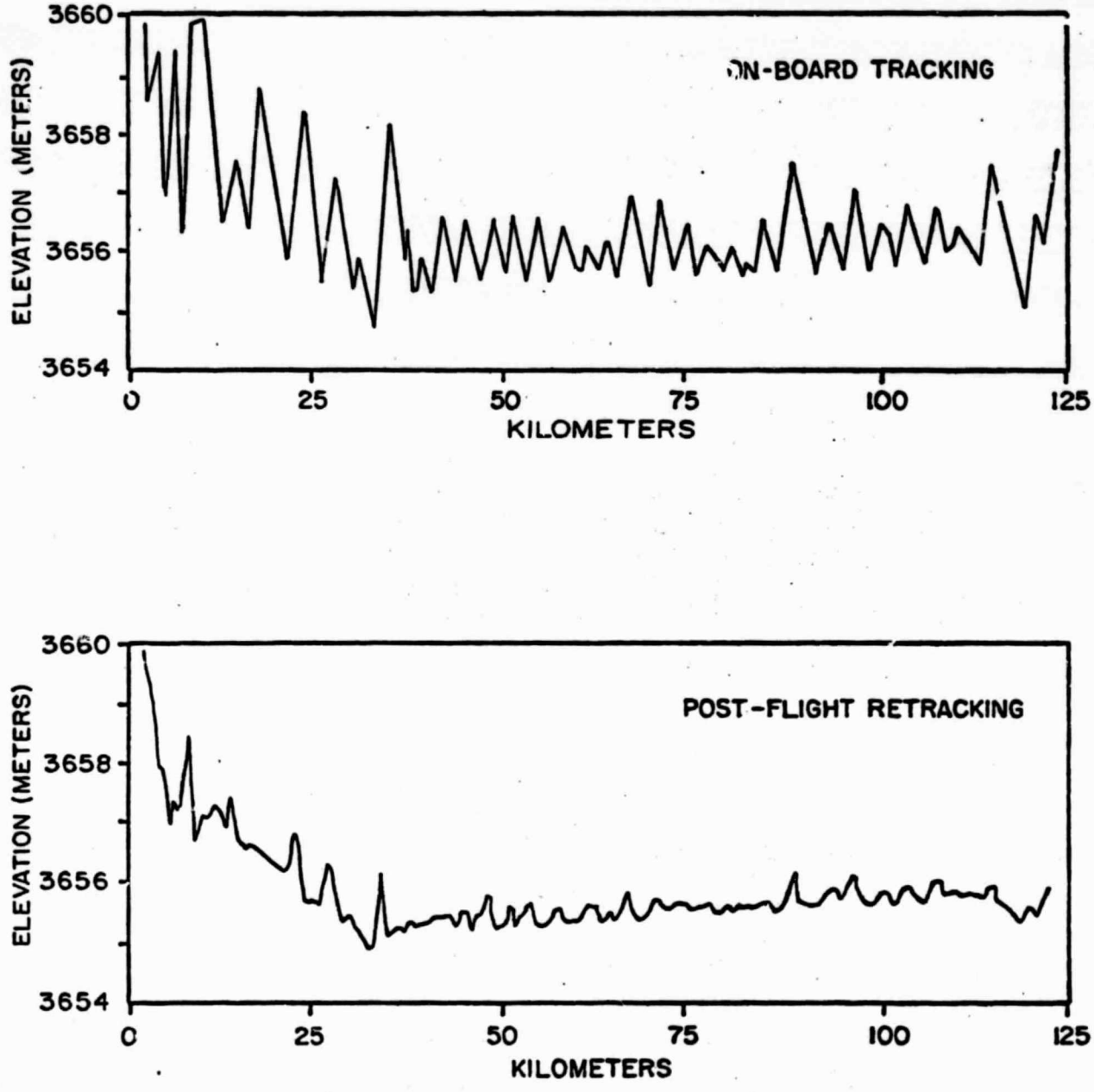

Figure 5 - Seasat Orbit 277 Altimeter Retracking Comparison for 125 km Across Salar de Uyuni.

Uyuni is the result of an anomalous or atypical waveform with two peaks as shown in Figure 6. Further examination reveals that the second peak is representative of the expected ground level. The source of the earlier peak is not known, although it probably represents an elevated surface feature. Even with the inclusion of the data spikes, the retracking is observed to significantly improve the computed surface elevations derived from the satellite altimeter measurements.

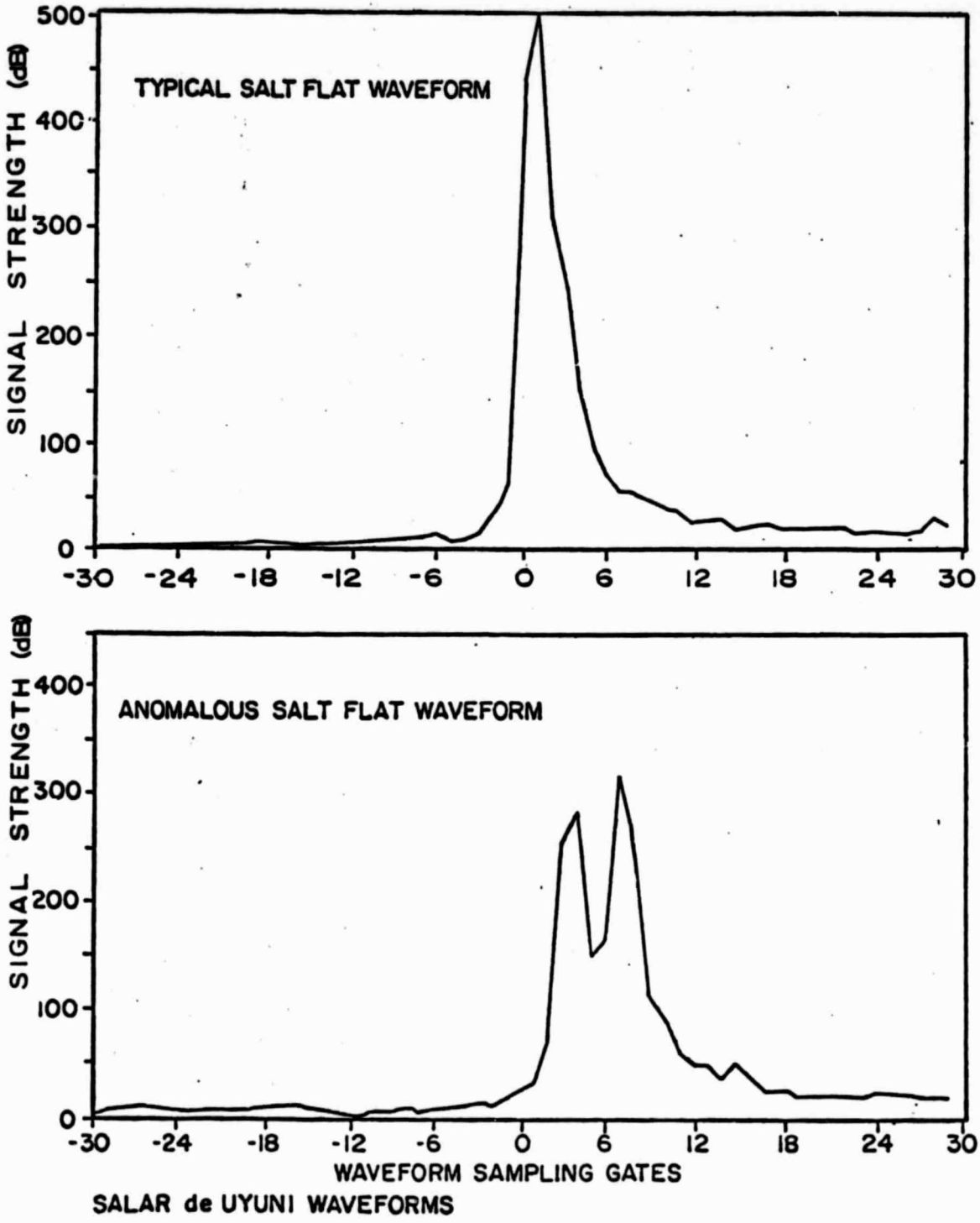

Figure 6 - Typical and Anomalous Seasat Waveforms from Salar de Uyuni.

ANDEAN SALAR RESULTANT SURFACE ELEVATIONS

The retracked altimeter measurements for orbits 277, 521, and 765 were zero-set on the South Atlantic Ocean after rectifying the surface heights for open-ocean and solid-earth tides (Schwiderski model). The altimeter-derived surface elevations in the vicinity of Salar de Uyuni and Salar de Coipasa were then computed. Initially comparing the Seasat surface elevations with elevations around the Salar de Uyuni margin provided by the Servicio Geologico de Bolivia, via Carter (personal communication, 1980), it is evident that the GEM-8 geoid-ellipsoid separation values are not appropriate. Using all three Seasat passes and simultaneously fitting the altimeter-derived surface heights to the Bolivian ground truth, the geoid height and slope at -20° latitude, -67.3° longitude is computed to be 52.1 m with a slope of -.0086 m per km towards the northwest. The GEM-8 model's height and slope for the same area is 54.2 m with a slope of +.0016 m per km. This discrepancy is well within the expected GEM-8 error bounds for this part if the world and may actually be the result of differences in reference ellipsoids.

The computed geoid height and geoid slope were then uniformly applied to the retracked Seasat-derived surface heights for orbits 277, 521, and 765. Where the groundtrack for orbit 521 crossed the groundtrack for orbit 485, just

north of -19°S latitude, the extrapolated geoid height is 50.9 m. In the absence of ground truth, the geoid slope for orbit 485 across the Salar de Coipasa was assigned a value of zero.

The resultant surface elevations across the two salars are shown in Figure 7 for every fifth Seasat measurement. The intervening points have been computed and are available upon request. It is observed from Figure 7 that the surface of Salar de Uyuni slopes upward towards the north at a rate of only about 1 m per 40 km. Superimposed on the trend are a few small areas of 10 - 30 cm lower elevation, where, due to prolonged surface ponding, potassium and lithium salts may be concentrated.

The elevations across Salar de Coipasa in the upper left of Figure 7 reveal that its lower elevations are towards its center.

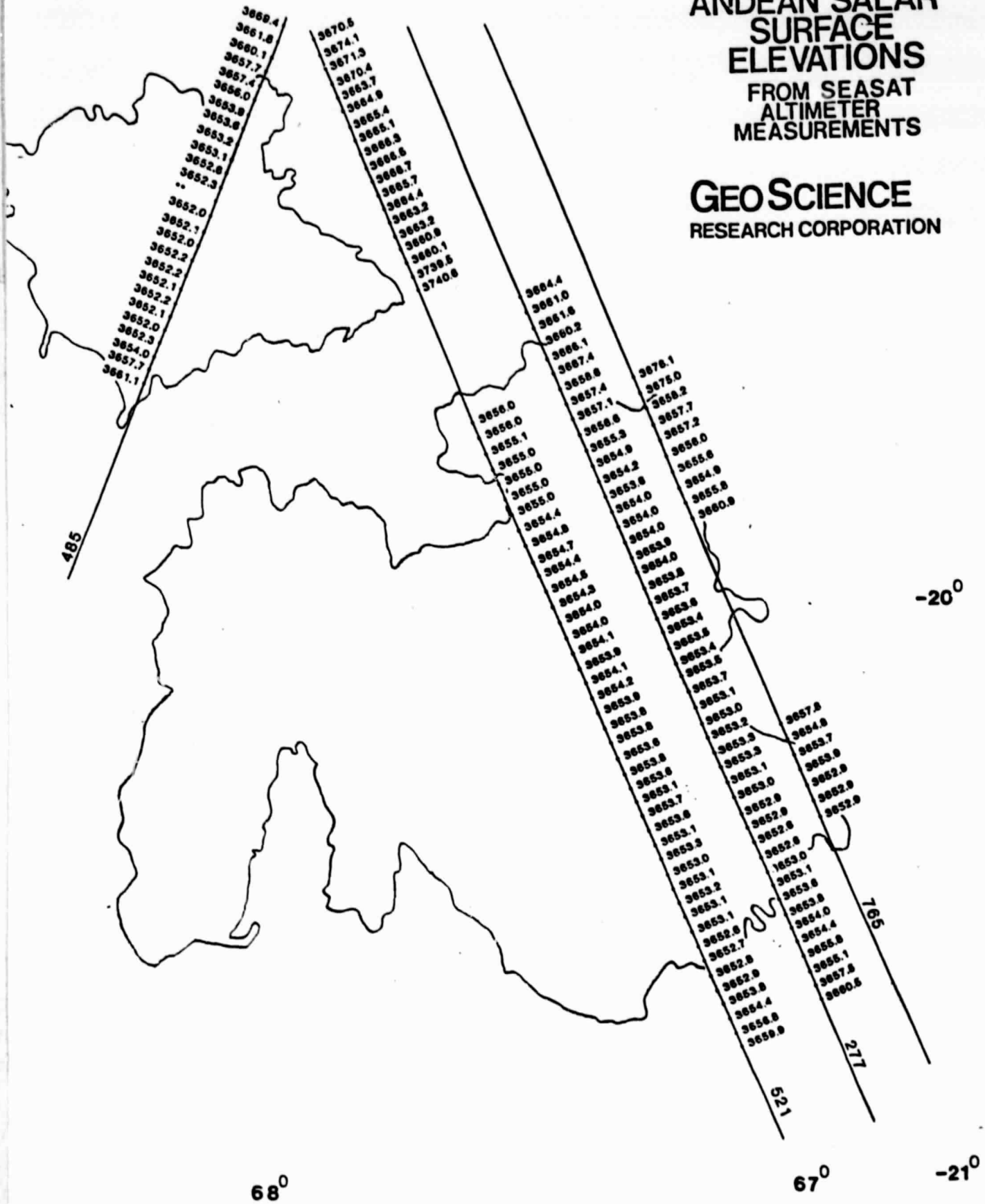

Figure 7 - Surface Elevations in Meters.

ALASKA

Due to the current U. S. interest in the expansion of large-scale mapping coverage in Alaska, the Seasat altimeter performance over the state was reviewed to assess the potential Seasat contribution. Altimeter waveforms and derived surface elevations were analyzed for 50 Seasat passes well-distributed across the state. Alaska's topography is predominantly mountainous with surface elevation rates far in excess of the altimeter tracker's capability to keep the return waveforms within the sampling gates.

There are two areas of Alaska, however, over which the Seasat altimeter consistently maintained lock and apparently could provide complementary vertical control for large-scale mapping.

The first of these areas is the North Slope (shown in Figure 8), north of Brooks Range and extending northward from 70°N latitude to the Arctic Ocean. This area is approximately 25,000 km^2 in size (slightly larger than New Hampshire); the surface is fragile tundra. The North Slope area also contains the Naval Petroleum Reserve No. 4. A typical Seasat altimeter waveform from the North Slope is plotted in Figure 9; correlation of this waveform with the best maps available shows that the peak power near gate +1 is from nadir while the peaks at gates +5 and +14 are apparently off-nadir reflections from two

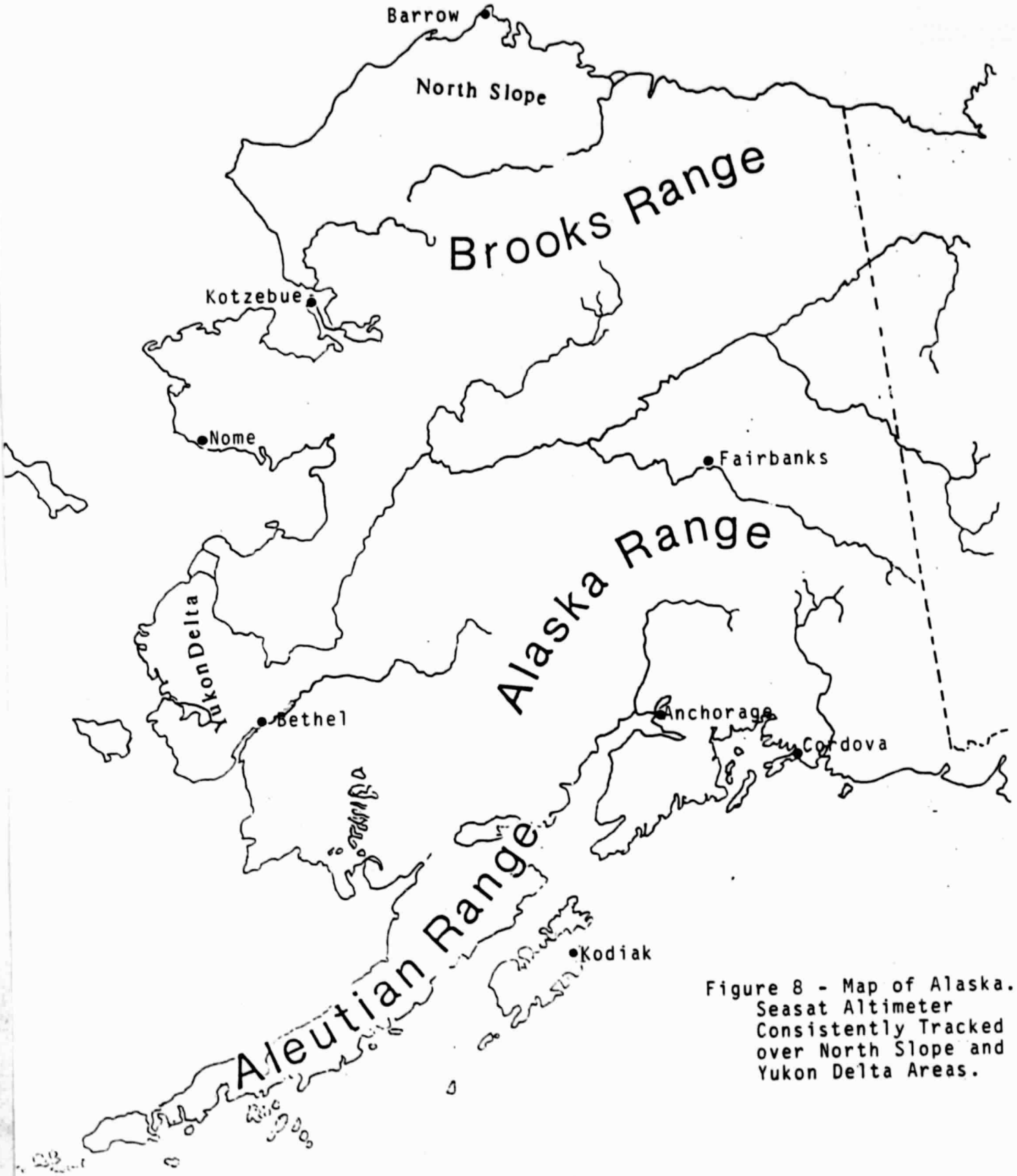

Figure 8 - Map of Alaska. Seasat Altimeter Consistently Tracked over North Slope and Yukon Delta Areas.

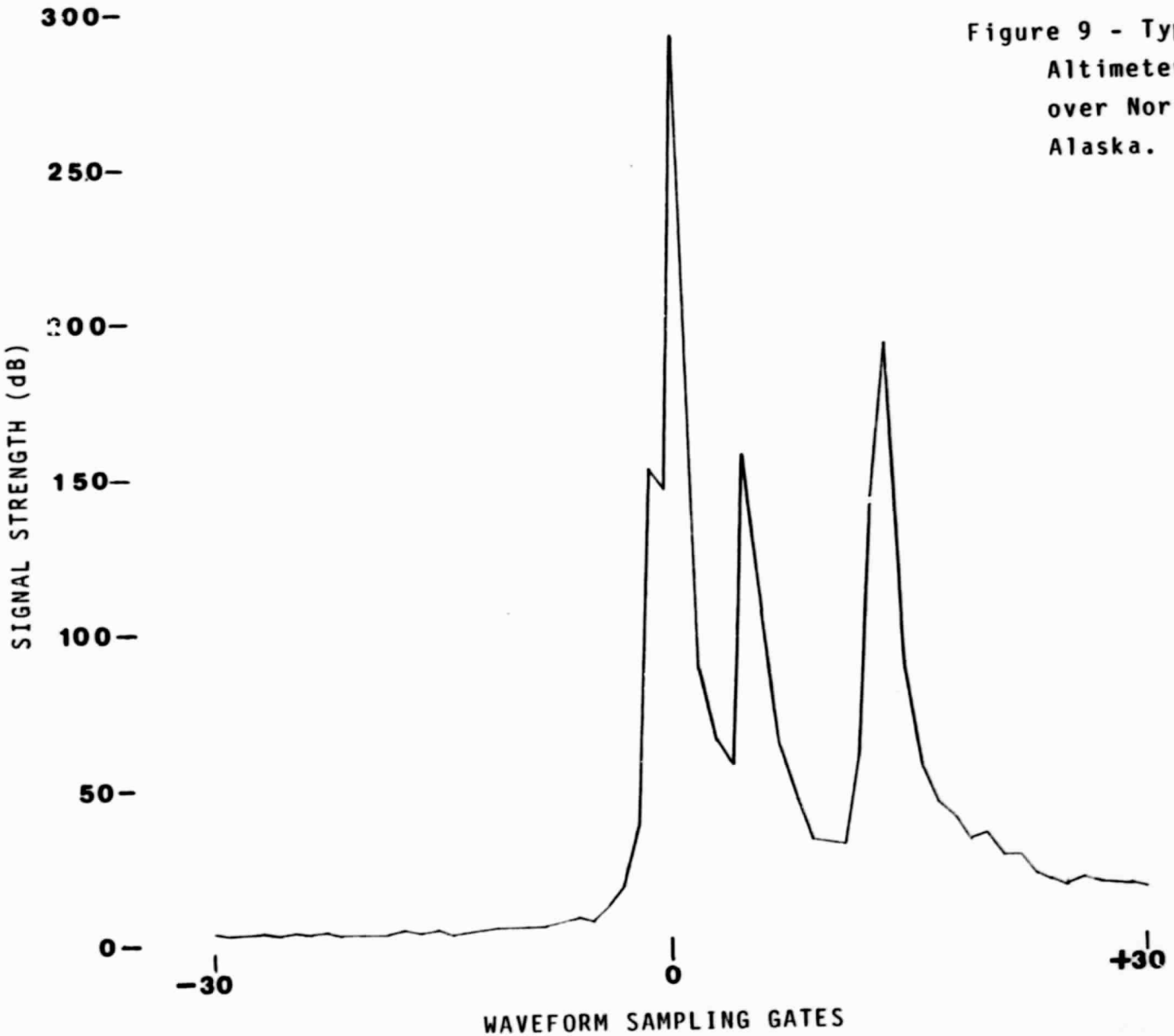

Figure 9 - Typical Seasat Altimeter Waveform over North Slope of Alaska.

of the very numerous nearby lakes.

Due to the paucity of vertical control in the North Slope, the accuracy of the Seasat-derived elevations was assessed by:

a) retracking the altimeter data
b) zero-setting the measurements on the Arctic Ocean
c) examining the altimeter-derived surface elevations for consistency near the groundtracks' intersections.

An example of internal consistency at the intersection of groundtracks is shown in Figure 10. In this Figure, the straight lines represent the groundtracks while the dots are at the altimeter nadir for each measurement (700 m spacing). The computed surface elevation in meters is notated beside each dot; the values in parenthesis are the surface elevations in meters from the on-board tracker prior to retracking. The retracked elevations for revolutions 176 and 551 both indicate an elevation rise towards the east.

The second area of Alaska where the Seasat altimeter consistently maintained lock is the Yukon Delta, also shown in Figure 8. This is a low-lying area south of Norton Sound along the west coast of Alaska, which encompasses about 23,000 km^2 and includes the Clarence Rhode National Wildlife Range. Figure 11 is a sample Seasat groundtrack intersection

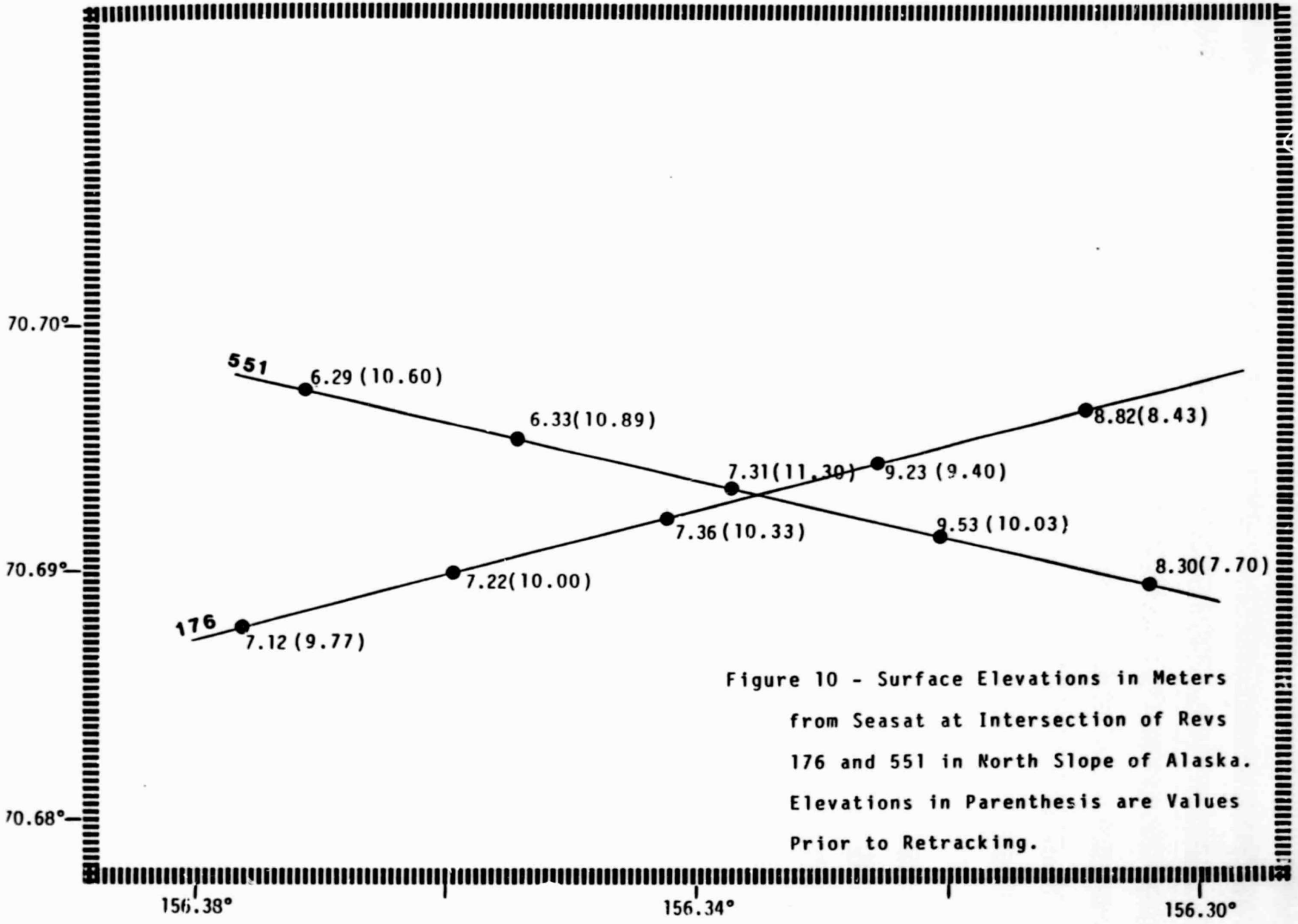

Figure 10 - Surface Elevations in Meters from Seasat at Intersection of Revs 176 and 551 in North Slope of Alaska. Elevations in Parenthesis are Values Prior to Retracking.

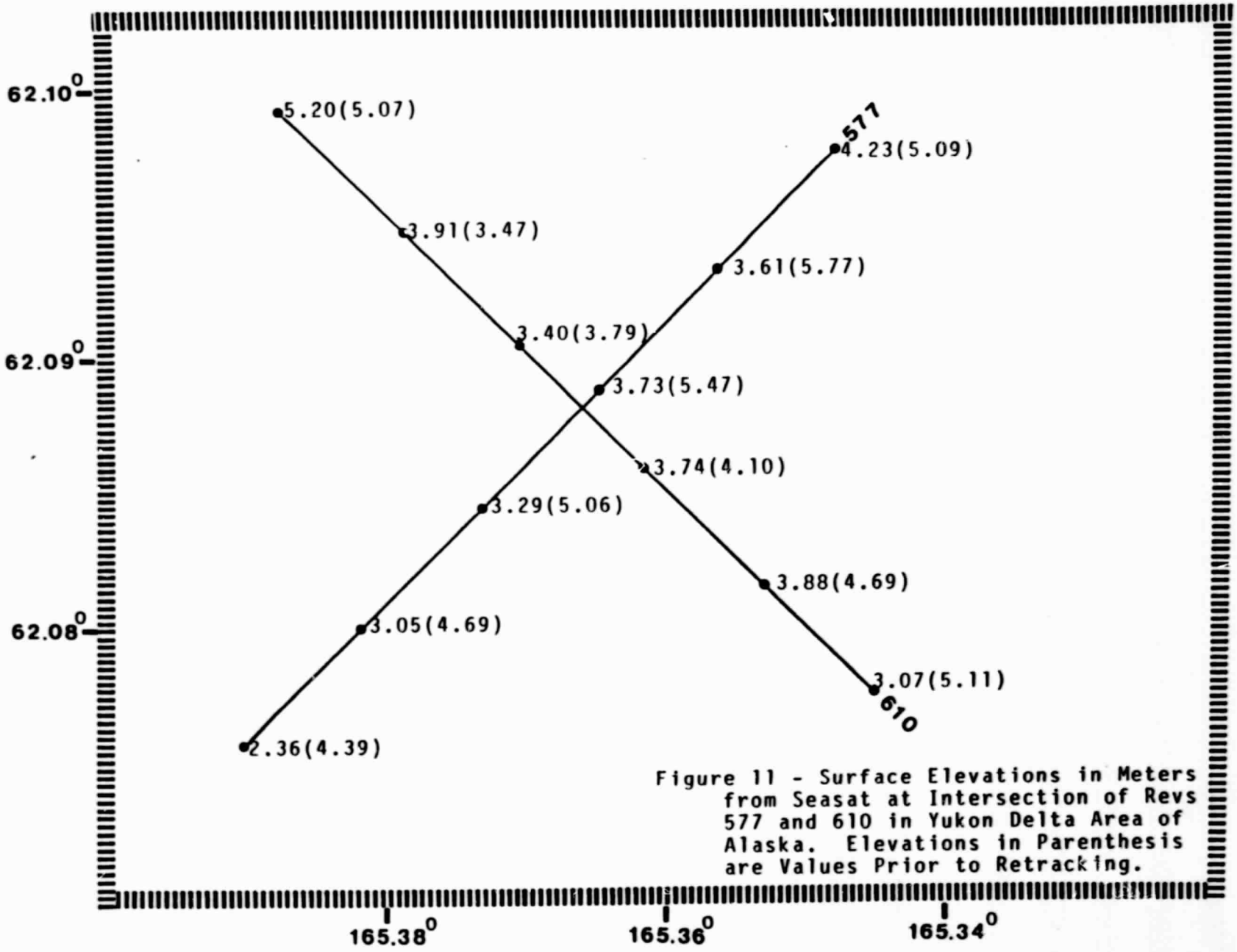

Figure 11 - Surface Elevations in Meters from Seasat at Intersection of Revs 577 and 610 in Yukon Delta Area of Alaska. Elevations in Parenthesis are Values Prior to Retracking.

over the Yukon Delta with both passes, revolutions 577 and 610, indicating lower terrain elevations to the south. Both passes were zero-set on the Bering Sea, just to the west of the Delta, to remove the orbital H error. The value in parenthesis is again the surface elevation prior to retracking and here, also, the elevation consistency at the intersection is enhanced by retracking.

All the retracked intersections examined over both the Yukon Delta and North Slope have exhibited similar elevation agreement, leading to the conclusion that Seasat altimetry could greatly assist the U. S. Government in their large-scale mapping of Alaska.

Over the areas of more rugged terrain in Alaska (the majority of the State), the altimeter status bit occasionally indicated valid tracking data, generally for one to four seconds at a time. Correlations with maps showed that the altimeter-derived elevations over the rugged topography were consistently low, indicating that the altimeter was locked-on to less rugged off-nadir targets such as snow fields and lakes. In the Prince William Sound near Cordova, for example, the altimeter indicated that valid tracking data was acquired over the off-shore islands. Examination of the waveforms and computed surface elevations reveals that the altimeter continued to track the Sound's water surface, even while the nadir point was at the middle of the island.

SOUTH-CENTRAL ARIZONA

Arizona has the highest population growth rate (25% increase from 1970 to 1975) of any state in the nation. The combination of a dry climate and greatly increased water usage in the area has resulted in dramatic lowering of the water table in central Arizona as much as 140 m, causing widespread land subsidence and earth fissures. The problem is most severe in the area of south-central Arizona around Eloy, where ground-water declines have caused approximately 1,200 km^2 of land to subside more than 30 cm since 1934, with a maximum measured subsidence of 3.8 m (Laney, et al, 1978) (Jachens and Holzer, 1979). The subsidence in this region has been attributed to compaction of unconsolidated alluvium ranging in thickness from 0 - 750 m. The locations of water level declines and earth fissures in south-central Arizona are shown in Figure 12 from Winikka and Wold (1977).

The releveling in this area has been very limited; as a result, the extent of the subsidence is not known. Brooks (1981) documents the analysis of two GEOS-3 and one Seasat satellite radar altimeter passes through this area which add to the knowledge of regional subsidence. The groundtracks of the three satellite altimeter passes are shown also in Figure 12. This report concentrates on the results from Seasat revolution 502 on August 1, 1978.

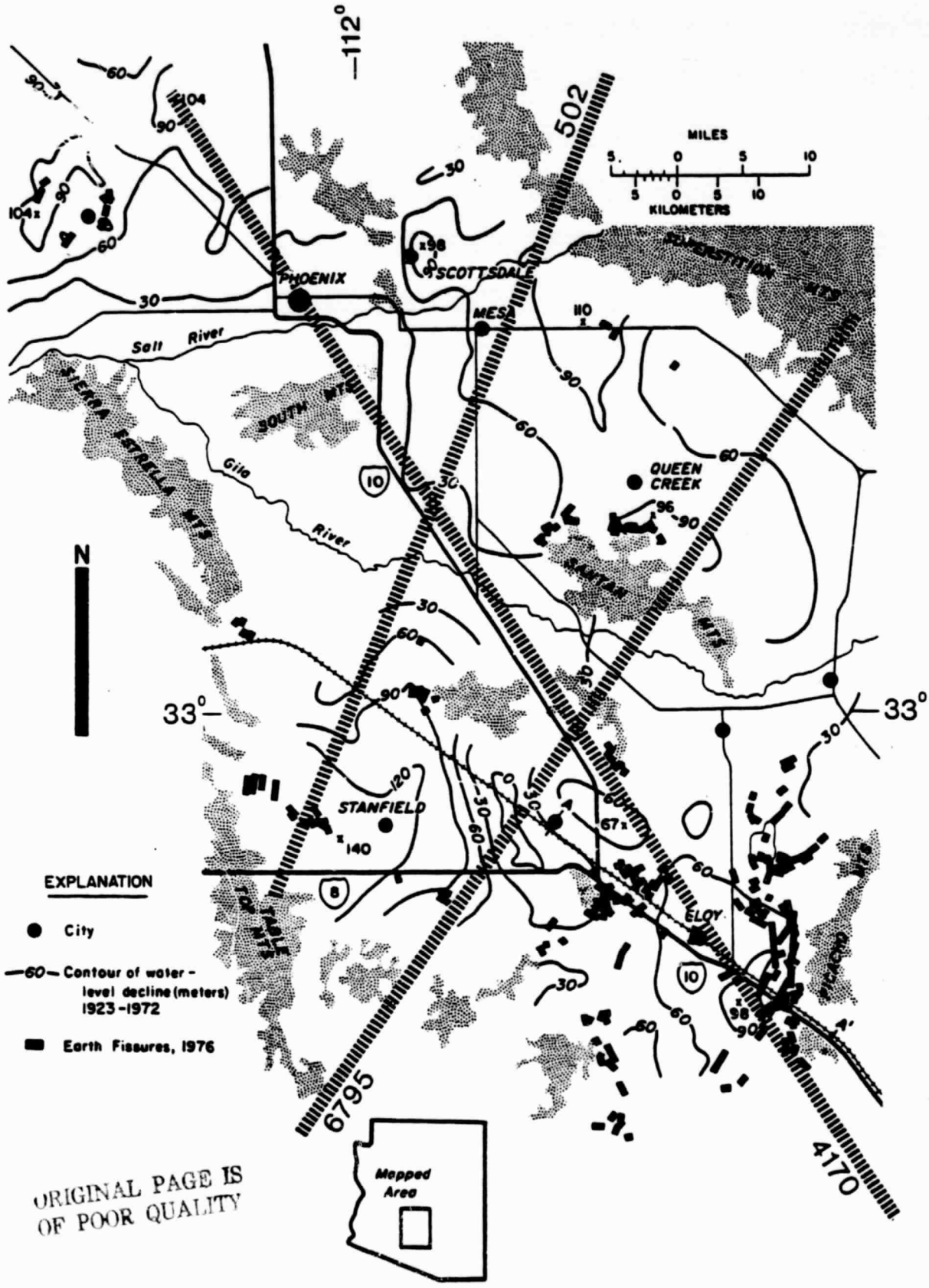

Figure 12 Satellite Altimeter Groundtraces in South-Central Arizona on a Basemap from Winikka and Wold (1977) Depicting Water-Level Declines and Earth Fissures.

The Seasat data were zero-set on the Pacific Ocean just to the west of Baja California at latitude 27.20°N, longitude 115.00°E with a tidal correction applied. The satellite groundtrace was located, point-by-point, on the most current USGS 1:24,000 maps. The map elevations were then correlated with the altimeter-derived elevations, and the height differences were ascribed to land subsidence between the times of the map survey and the altimeter overflight.

Seasat Orbit 502 traversed the subsidence study area in a northeast-to-southwest direction (right-to-left in Figure 13). The top portion of the Figure illustrates that the terrain profile from the 1:24,000 maps was very favorable for altimeter tracking. In spite of this, the Seasat altimeter utilized 30 km of smooth terrain during its acquisition cycle.

Seasat acquired terrain measurements from 33.25°, southwest of Chandler, to 32.97° latitude. Map coverage for the Seasat altimeter was:

Map Name	Scale	Date	Contour Interval	Latitude Coverage
Gila Butt NW	1:24,000	1952	3.0m(10ft)	33.25°-33.13°
Sacaton Butte	1:24,000	1952	3.0m(10ft)	33.13°-33.03°
Maricopa	1:24,000	1952	3.0m(10ft)	33.03°-33.00°
Antelope Peak	1:24,000	1963	7.6m(25ft)	33.00°-32.97°

The correlation of the altimeter measurements and the maps

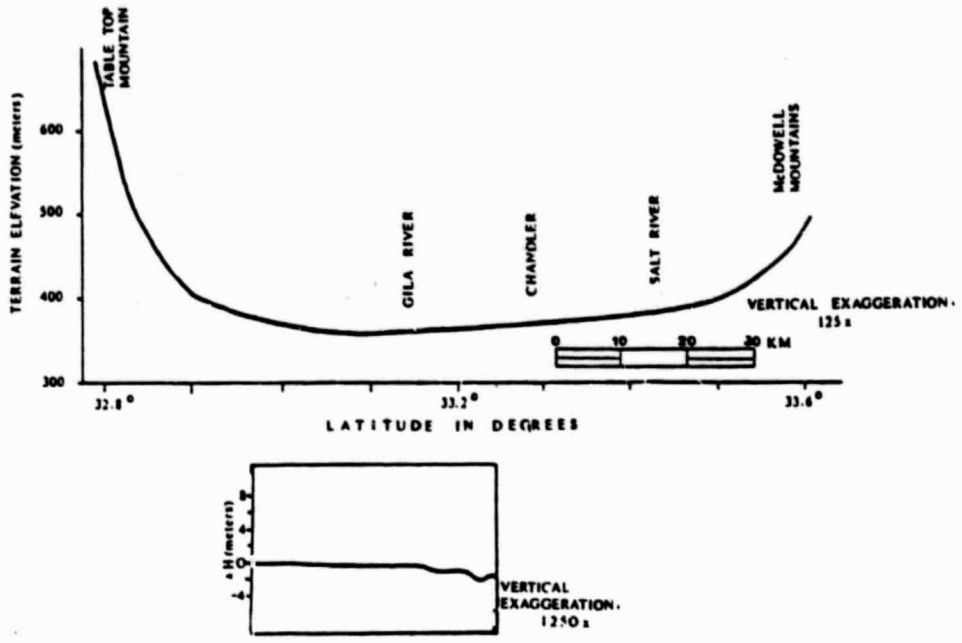

Figure 13 - Top: Terrain Profile for Seasat Orbit 502 Altimeter Overflight.

Bottom: Altimeter-Derived Terrain Elevations Minus Map Elevations.

indicates the presence of subsidence from the beginning of data lock-on, 33.25°, to 33.15° latitude. Subsidence is observed to be as large as 2.0 m. There is no known corroboration leveling data in this area, but as shown in Figure 12, this Seasat groundtrack intersected the groundtrack for GEOS-3 Orbit 4170. Both altimeters were tracking the terrain at the intersection and both indicated that subsidence had occurred. Figure 14 shows, point-by-point, the altimeter-derived estimates of subsidence near the intersection plotted as a function of latitude and longitude. At the sub-satellite points closest to the groundtracks' intersection, the subsidence estimates agree to the 0.2 m level.

From 33.15° latitude towards the southwest, there was no indication of subsidence. The Seasat altimeter lost lock at the terrain rise caused by Table Top Mountain.

Except for the rather long time required for acquisition, Seasat performed well over this area as the elevations derived from the retracked Seasat waveforms appear to be quite accurate.

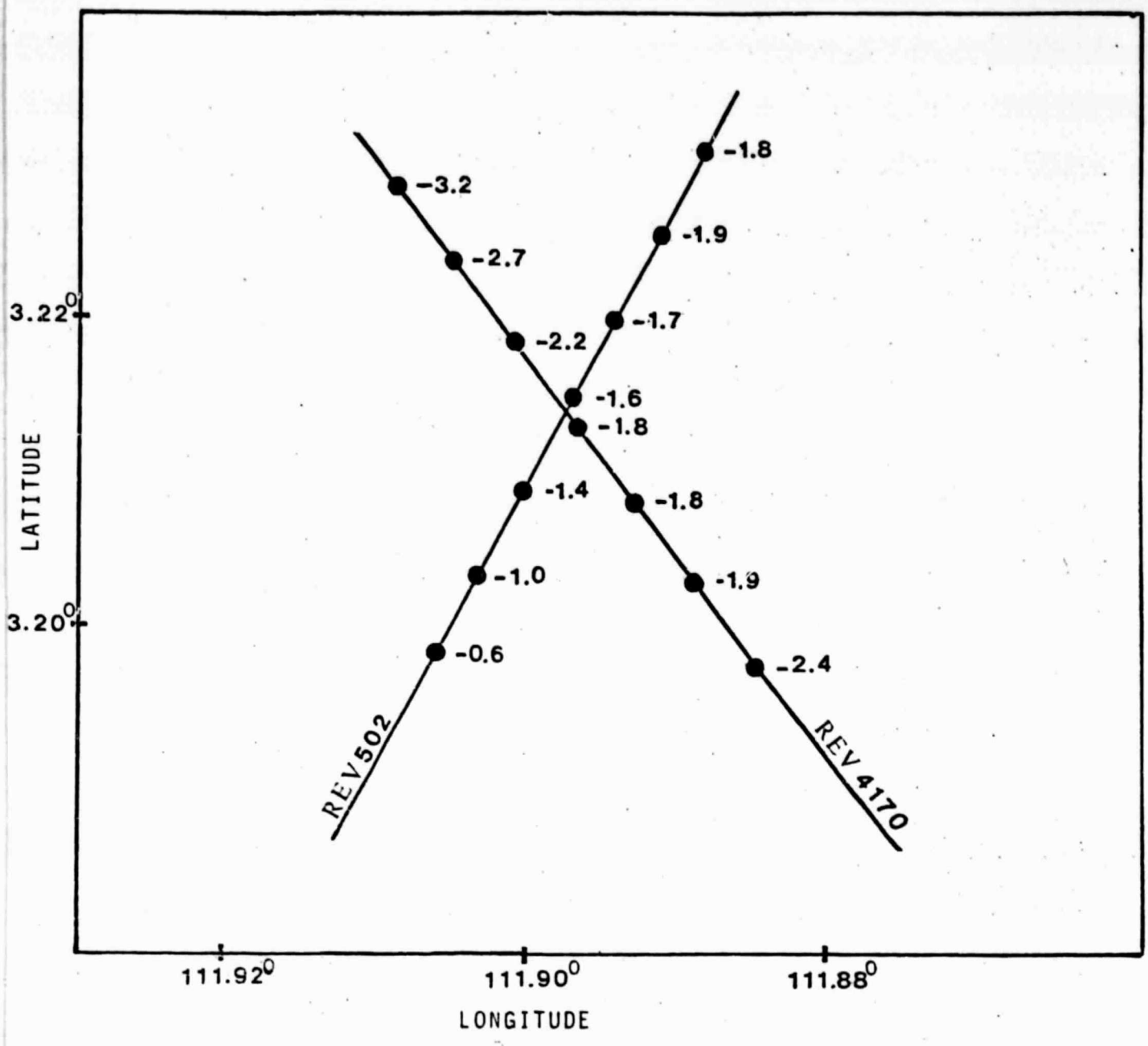

Figure 14 - Altimeter-Derived Subsidence Measurements Near the Intersection of GEOS-3 Orbit 4170 and Seasat Orbit 502 Groundtracks.

IMPERIAL VALLEY OF CALIFORNIA

The Imperial Valley of California is known geologically as the Salton Trough and is the northern extension of the Gulf of California structure, a rift at the juncture of the North American and Pacific plates. The Imperial Valley has sustained more moderate to small earthquakes than any other area along the San Andreas Fault System.

The monitoring of vertical crustal movements in this area is of interest not only because of the active faults, but also because of the area's geothermal anomalies. Future land subsidence is anticipated in this area due to the planned extraction of geothermal steam. Significant subsidence would have an adverse effect on this area due to the altered gravity flow of irrigation water needed for agriculture, the lifeblood of the Valley.

To assess the potential of satellite altimetry assisting in the subsidence monitoring, the altimeter data from Seasat revolution 523 on the eastern edge of the Imperial Valley were correlated with 1:24,000 maps. The groundtrack for revolution 523 is depicted in Figure 15. The satellite traversed from the southeast to northwest, passing over sandhills of the East Mesa prior to passing over the eastern part of the Valley. The groundtrack exited the Valley at about 33°10' latitude as it again overflew the East Mesa. The altimeter's status indicated "lock-on" for the entire length of the cross-hatched path shown

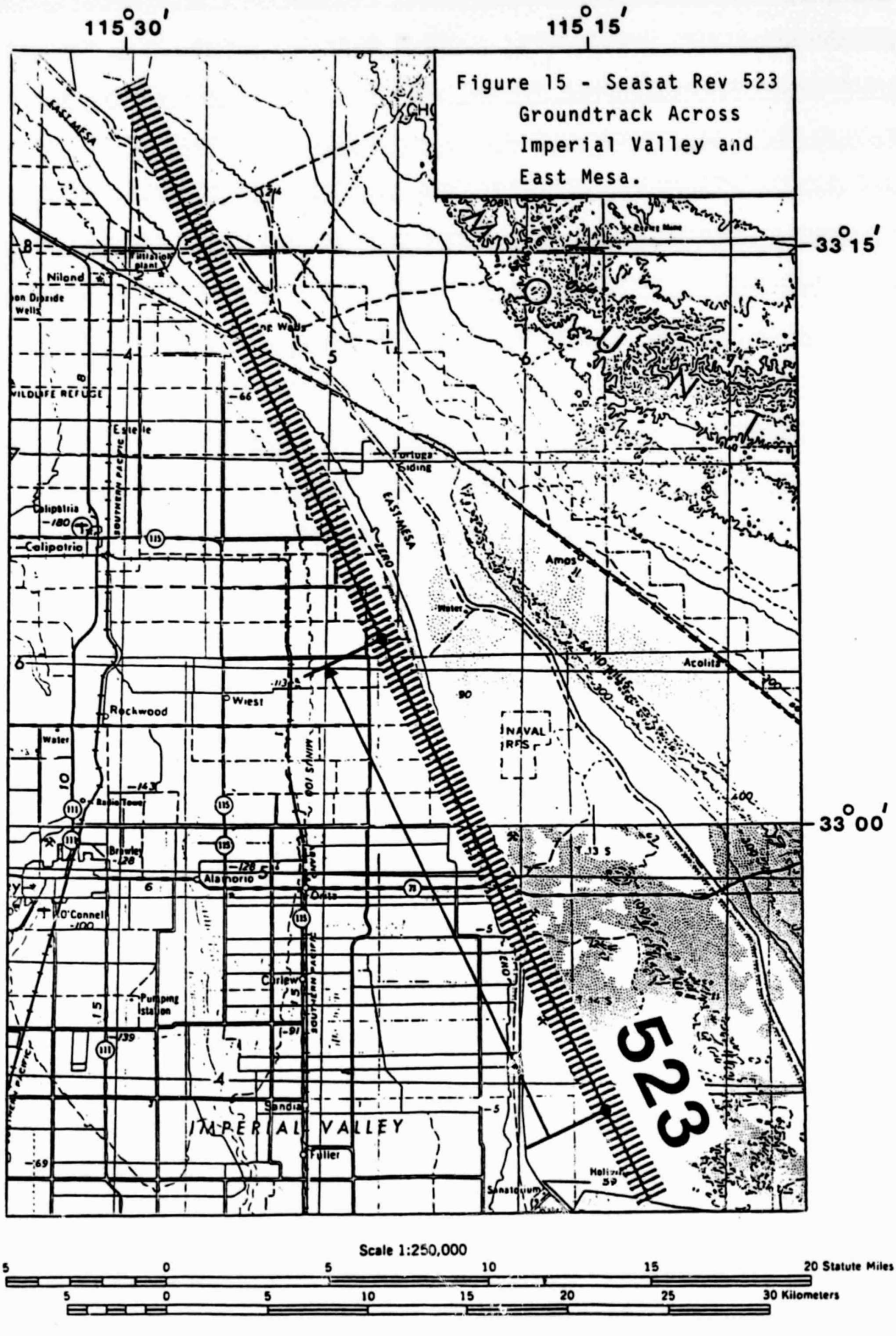
115°30′
115°15′
33°15′
33°00′
Figure 15 - Seasat Rev 523 Groundtrack Across Imperial Valley and East Mesa.
523
EAST MESA
Niland
Calipatria
Rockwood
Brawley
Alamorio
O'Connell
Pumping Station
Sandia
IMPERIAL VALLEY
Fuller
Sonalquum
Holtville
Tortuga Siding
Amos
Acolita
Wiest
NAVAL RFS
Scale 1:250,000
5 0 5 10 15 20 Statute Miles
5 0 5 10 15 20 25 30 Kilometers

in the Figure. The portion of the groundtrack successfully correlated with the 1:24,000 maps is that 25.5 km segment designated by the line with arrow, parallel to the groundtrack, in the bottom half of Figure 15. The maps utilized were:

Map Name	Scale	Date	Contour Interval
Holtville NE	1:24,000	1957	1.5m (5 ft)
Amos	1:24,000	1953	1.5m (5 ft)

The results of the correlation is shown in Figure 16 where the solid line is the profile from the maps, the dashed line represets the computed surface elevations from the on-board tracker, and the dots are surface elevations resulting from retracking the waveforms. The retracking significantly improves the computed surface elevations. The satellite direction in this Figure is right-to-left. The on-board tracker performed fairly well over the East Mesa, on the right in Figure 16. Once past the East Mesa, the on-board tracker's surface elevations diverge from the true (map) surface.

An examination of the terrain and the altimeter waveforms from this area is necessary to understand how the on-board tracker built up such a large divergence error. Figure 17 is an enlargement of a portion of the groundtrack area at a 1:24,000 scale; this is the transition area from the East Mesa to the Valley. The dots in Figure 17 are nadir points corresponding to the 0.1 second measurement rate. The letters A, B,

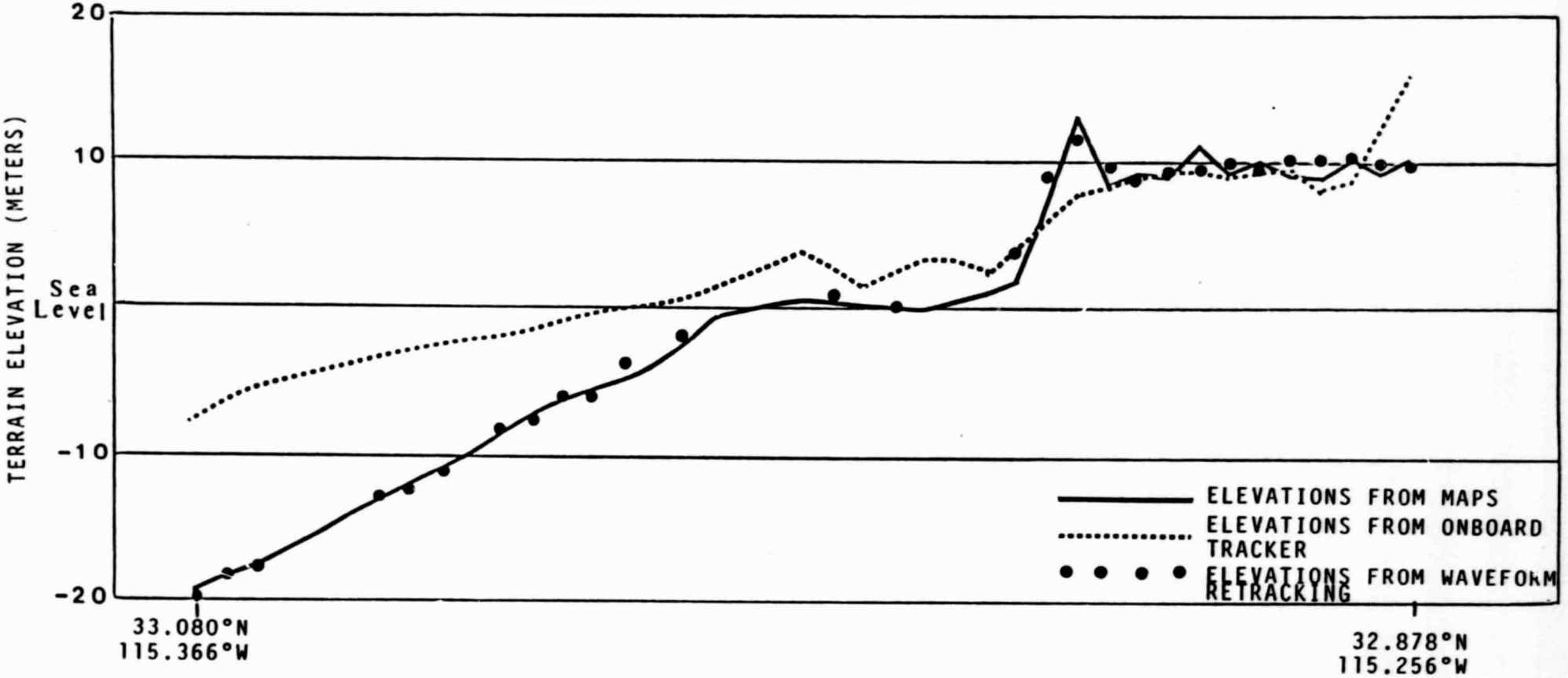

Figure 16 - Correlation of Altimeter-Derived Surface Elevations with 1:24,000 Map Elevations for 25.5 km Groundtrack Across East Mesa and Imperial Valley.

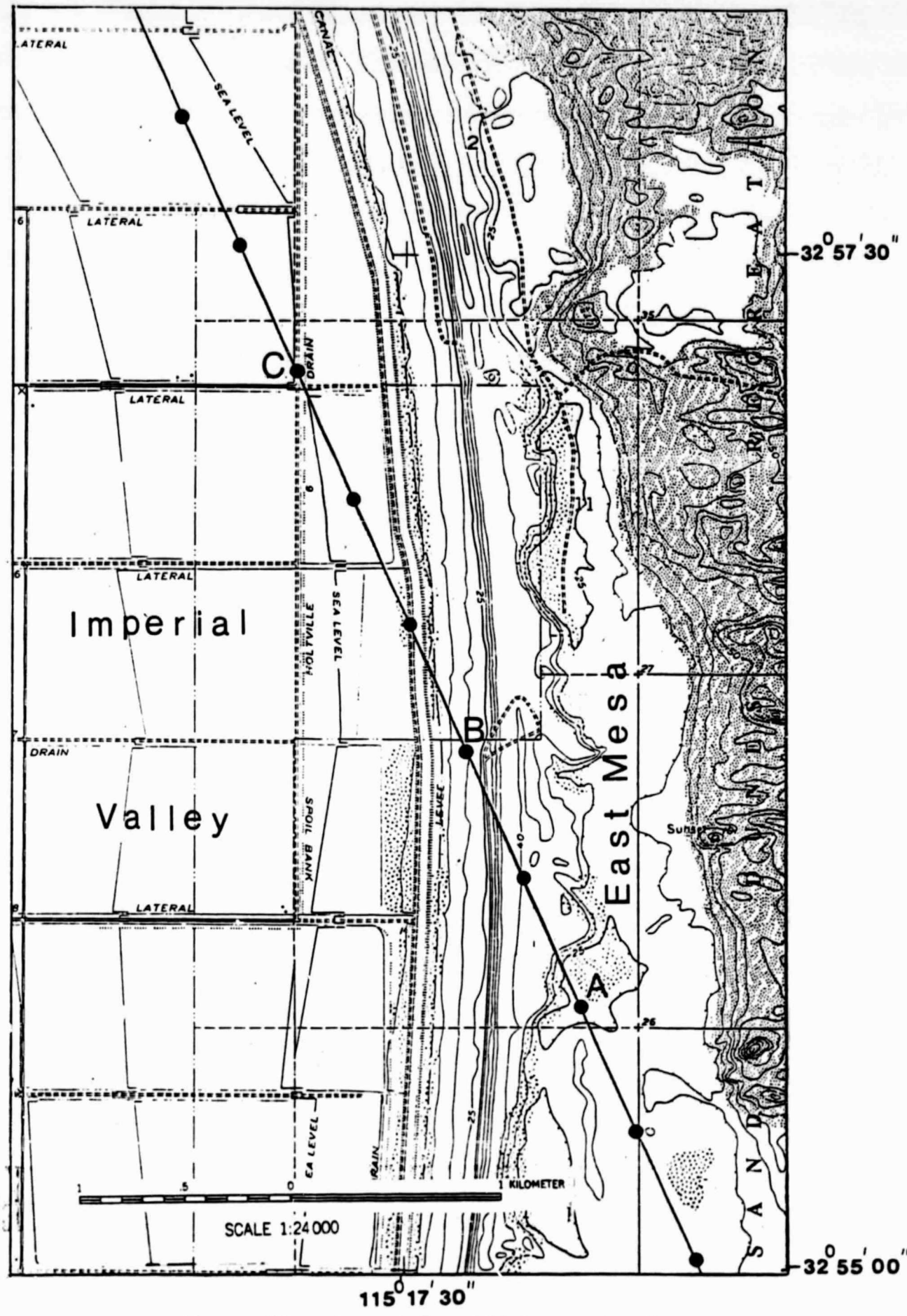

Figure 17 - Seasat Rev 523 Groundtrack Across East Mesa/Imperial Valley Transition.

and C in Figure 17 are locations of photographs taken in this area. Figure 18A is a photograph of the small rounded sand-hills on top of the East Mesa, corresponding to location A on Figure 17. The East Mesa/Valley transition area, corresponding to location B, is pictured in Figure 18B. The flatness of the Valley at location C is shown in Figure 18C. The altimeter waveforms for each of these three locations are plotted in Figure 19. Figure 19A is the waveform from location A on the East Mesa. The first return, starting at about gate -5, is a stretched-out signal from the hummocky Mesa; at gate +15, the specular Valley return appears.

The location B waveform, at the East Mesa/Valley transition, is shown in Figure 19B. Here the stretched-out Mesa return begins at gate -13; the beginning of the Valley return is seen at gate +10.

The waveform corresponding to location C is shown in Figure 19C. Even though the altimeter nadir is now over the Valley, the Mesa return still appears first in the waveform, followed by the Valley return. The reason for this positioning within the waveform is that the Mesa is still within the foot-print, being suffciently higher than the Valley, so the altimeter transmitted wavefront reflects first from the Mesa, then from the Valley.

Visual examination of subsequent waveforms reveals that the Seasat on-board tracker continued to track the first (Mesa) return over the remainder of the Valley. As long as the Valley

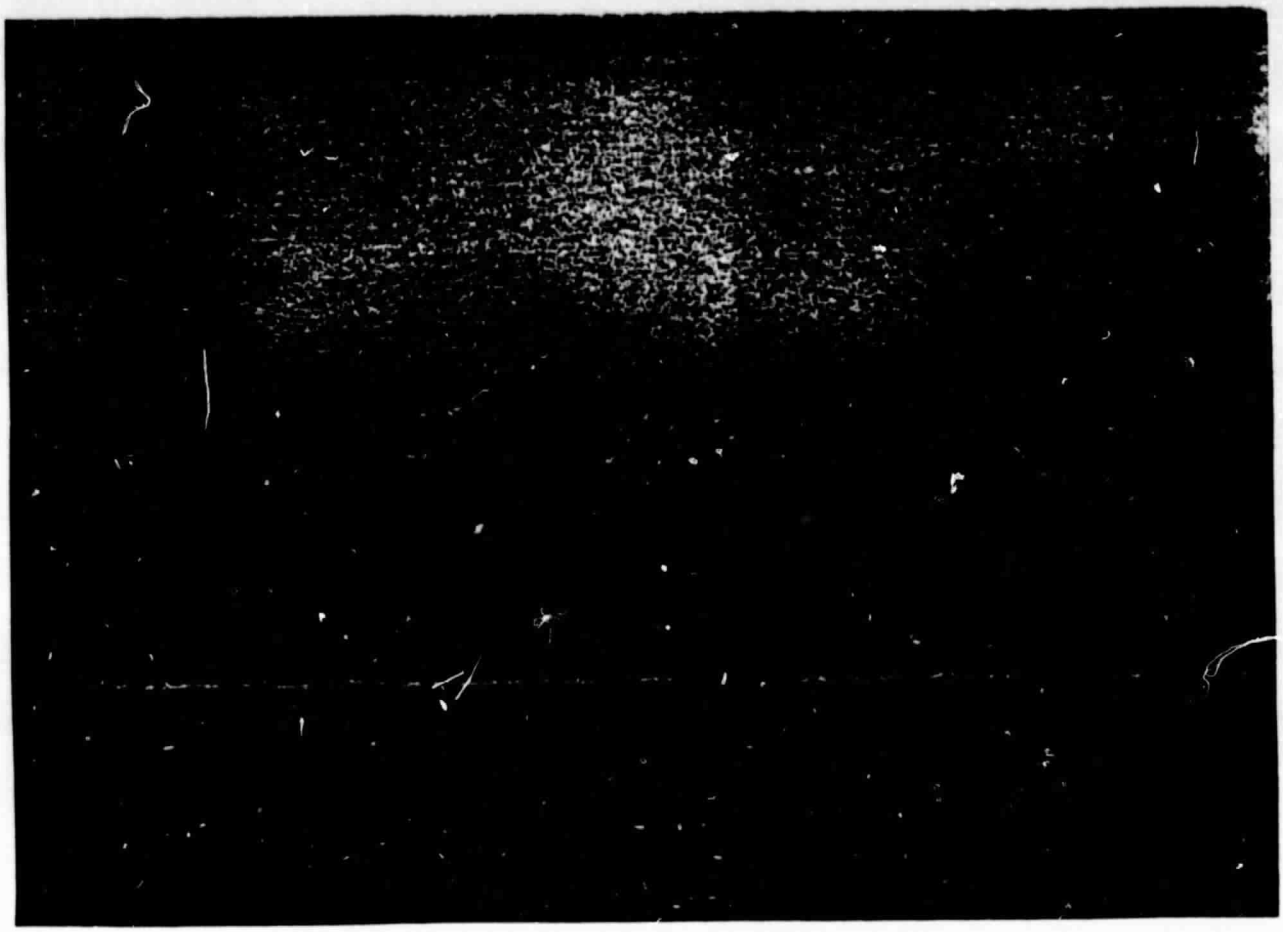

Figure 18A - Rounded Sand Hills on Top of East Mesa.

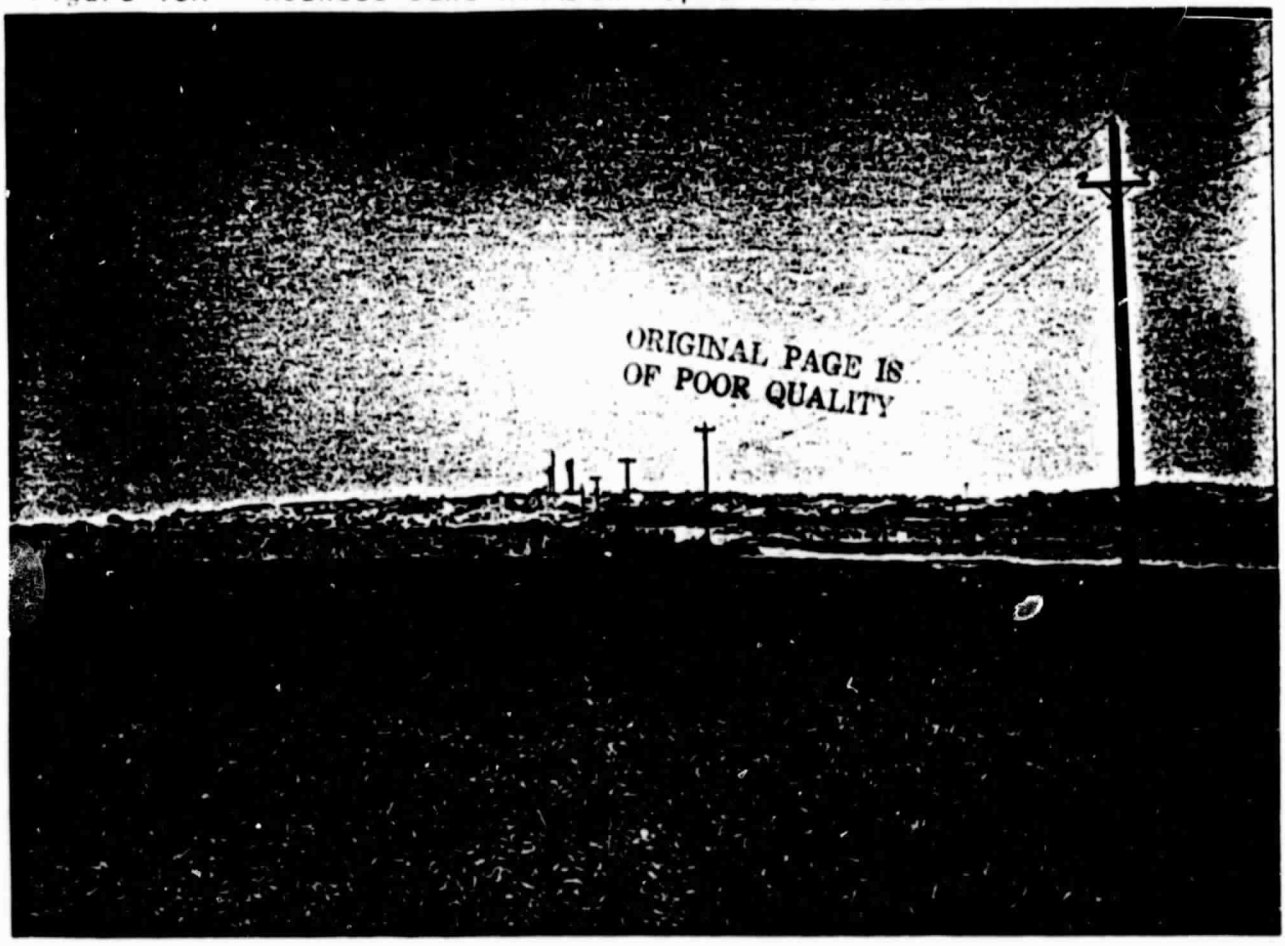

Figure 18B- Escarpment at East Mesa/Imperial Valley Transition.

Figure 18C - Flatness of Imperial Valley.

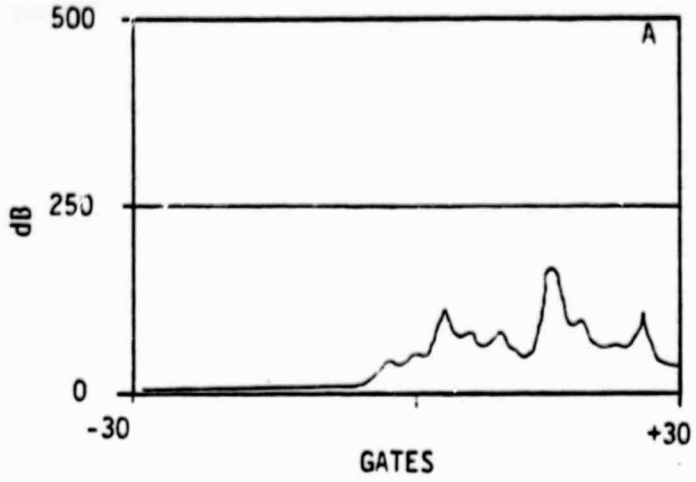

Figure 19A - Waveform at Location A on Top of East Mesa.

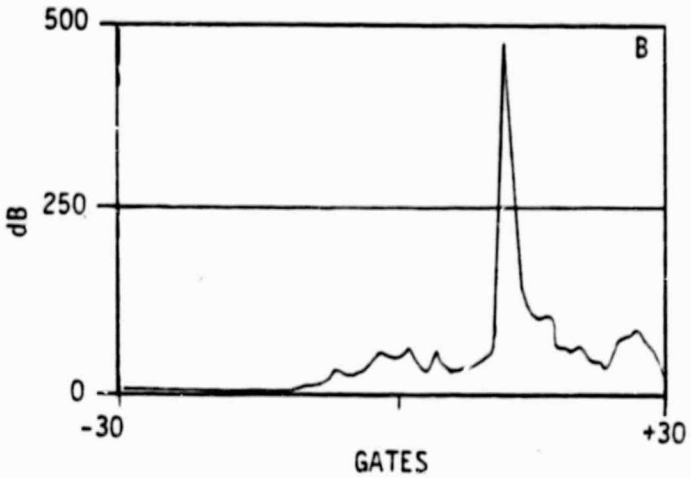

Figure 19B - Waveform at Location B at Mesa/ Valley Transition.

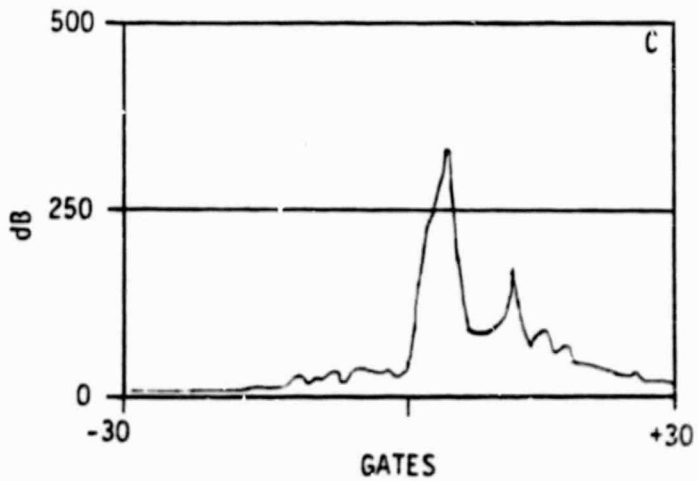

Figure 19C - Waveform at Location C Within Imperial Valley.

return remained in the waveform gates, it may be retracked at its 50% peak power point; the dots shown earlier in Figure 16 show the excellent results from this retracking. Where some dots are missing in Figure 16, the earlier Mesa return obscured the 50% peak power point of the Valley return, and retracking was not possible. At the far left of Figure 16, the retracking capability ceased because the Valley return was no longer in the sampled waveforms; it was to the right of gate +30.

The on-board tracker would have performed much better if the Mesa edge hadn't remained in the waveform; even here, however, retracking regained a sizable portion of the data.

Future Seasat-type satellite altimeters could effectively monitor subsidence in the Imperial Valley in a cost-effective manner. However, this type of rapidly changing terrain will require careful correlation of waveforms with the topography.

YUMA VALLEY OF ARIZONA

A geomorphological feature similar to the Imperial Valley's escarpment was encountered by a Seasat altimeter pass over the Yuma Valley in the southwestern tip of Arizona. As shown in Figure 20, the southeast-to-northwest groundtrack for Seasat revolution 767 traversed the Yuma Desert prior to descending into the Yuma Valley. Figure 21 is a cross-sectional view of this escarpment. The height of the Yuma Valley escarpment is 18 m compared with the 10 m escarpment height for the Imperial Valley.

The maps utilized for the altimeter analysis were:

Map Name	Scale	Date	Contour Interval
South of Yuma	1:62,500	1964	1.5 m (5 ft)
Somerton	1:24,000	1965	1.5 m (5 ft)
Gadsden	1:24,000	1965	1.5 m (5 ft)
Grays Well NE	1:24,000	1964	1.5 m (5 ft)

The altimeter/map comparison is shown in Figure 22 where the satellite direction is right-to-left. The altimeter's onboard tracker performed well over the Yuma Desert; however, as in the Imperial Valley analysis, the onboard tracker could not respond to the Desert-Valley transition, and continued to track the higher desert terrain.

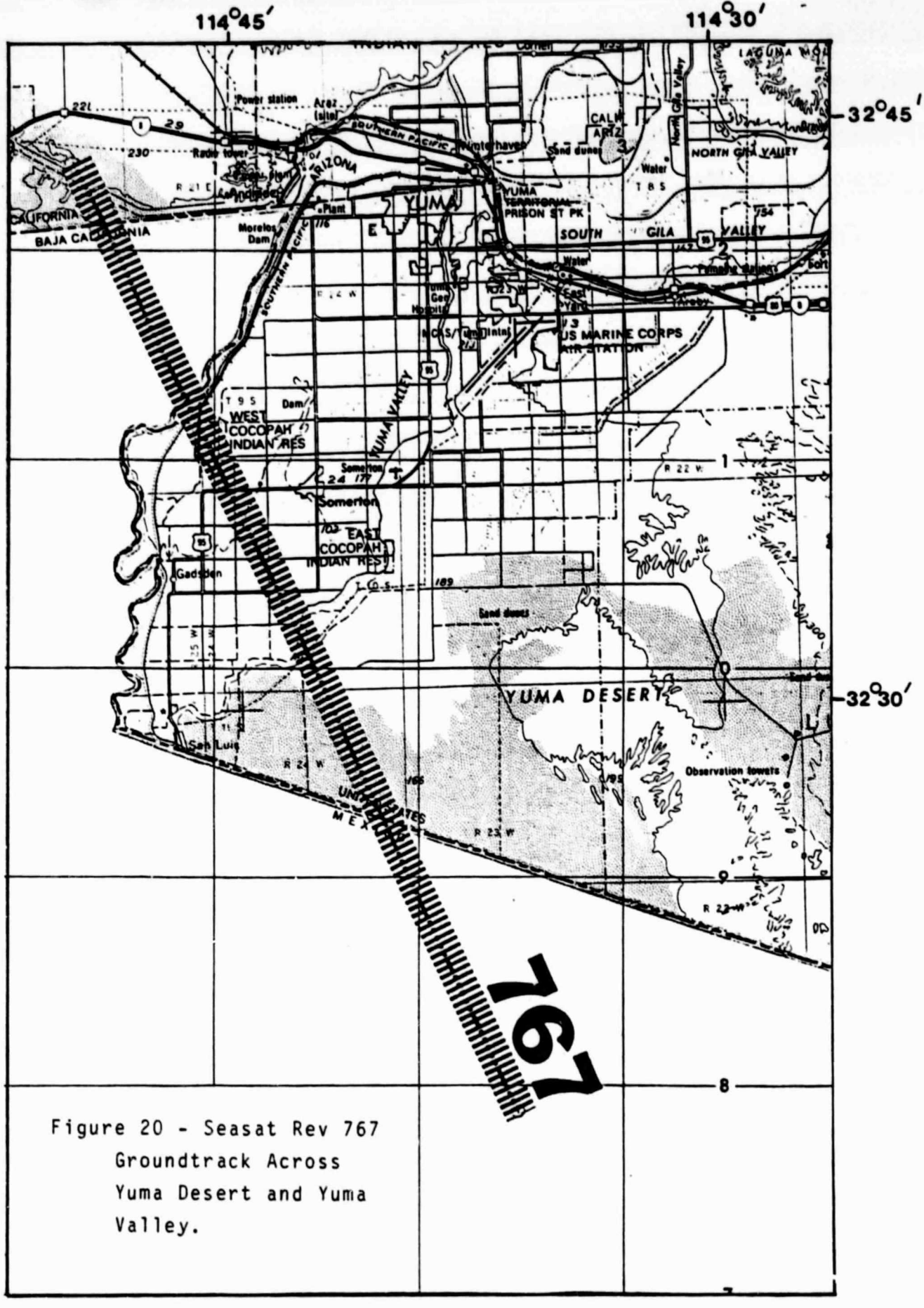

Figure 20 - Seasat Rev 767 Groundtrack Across Yuma Desert and Yuma Valley.

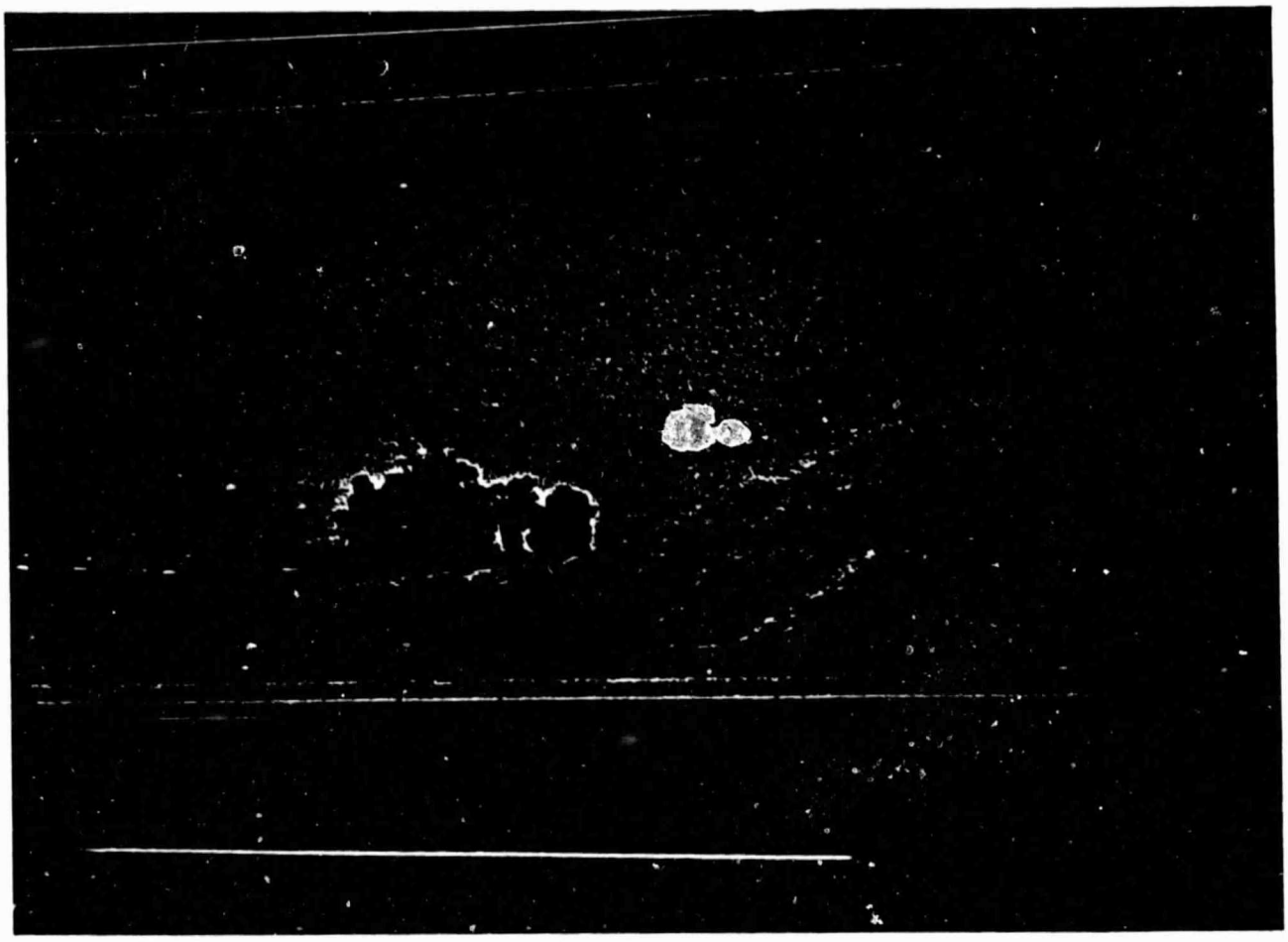

Figure 21- Escarpment at Transition Zone between Yuma Desert and Yuma Valley.

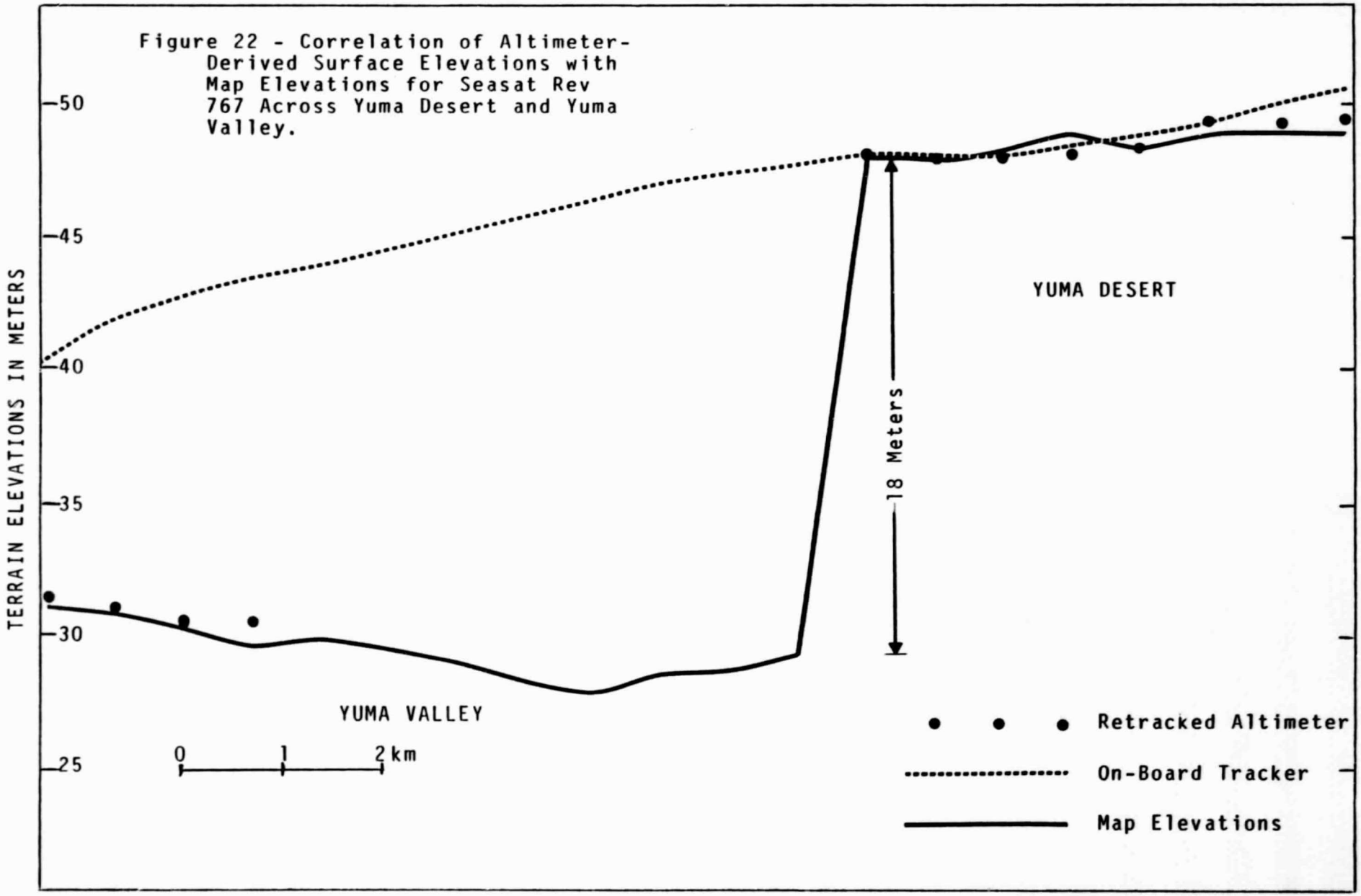
Figure 22 - Correlation of Altimeter-Derived Surface Elevations with Map Elevations for Seasat Rev 767 Across Yuma Desert and Yuma Valley.
TERRAIN ELEVATIONS IN METERS
50
45
40
35
30
25
YUMA DESERT
18 Meters
YUMA VALLEY
0
1
2 km
Retracked Altimeter
On-Board Tracker
Map Elevations

Because the height difference between the valley floor and the onboard tracker exceeds 14.05 m (30 gates x 46.84 cm/gate), the waveform return from the valley floor is not initially within the waveform sampling gates. There is no retracking possible until the height difference narrows to 14.05 m and the valley return appears. Once the valley return is available, the retacking results (shown by dots in Figure 22) are again within ±1 m of the map elevations.

A future satellite altimeter would need waveform sampling gates distributed over a wider time regime if step-functions such as this Desert-Valley transition were to be measured.

GREAT SALT LAKE DESERT

Seasat rev 574 approached the Great Salt Lake Desert from the northeast moving southwest as shown in Figure 23. The altimeter was not "locked-on" over Promontory Mountains, but as the satellite tracked toward the Great Salt Lake the terrain flattened. "Lock-on" was established approximately six km northeast of the lake and became very stable over the lake itself and the adjoining Great Salt Lake Desert to the southwest. The crosshatched portion of the ground track in Figure 23 represents the period of "lock-on".

The Seasat subsatellite points were plotted on USGS Utah maps Dolphin Island East, Gunnison Island N. E., Gunnison Island S. W., Strongs Knob, and Hogup Ridge South. These 1969 maps have a 1:24,000 scale with a primary contour interval of 20 feet with intermediate 5 foot contours. There is no 1:24,000 map for the area from 41.125° to 41.000° latitude.

Altimeter measurements at the rate of 10 per second with a groundtrack spacing of 700 meters were selected for analysis. The orbital radial error was compensated for by zero-setting the altimeter-derived elevations near the Southern Pacific railroad grade in the extreme northwestern corner of the Strongs Knob quadrangle.

Three discrete segments of the Seasat ground track are labelled in Figure 24; segment A begins over the Great Salt Lake and continues to the Southern Pacific Railroad, segment B begins at

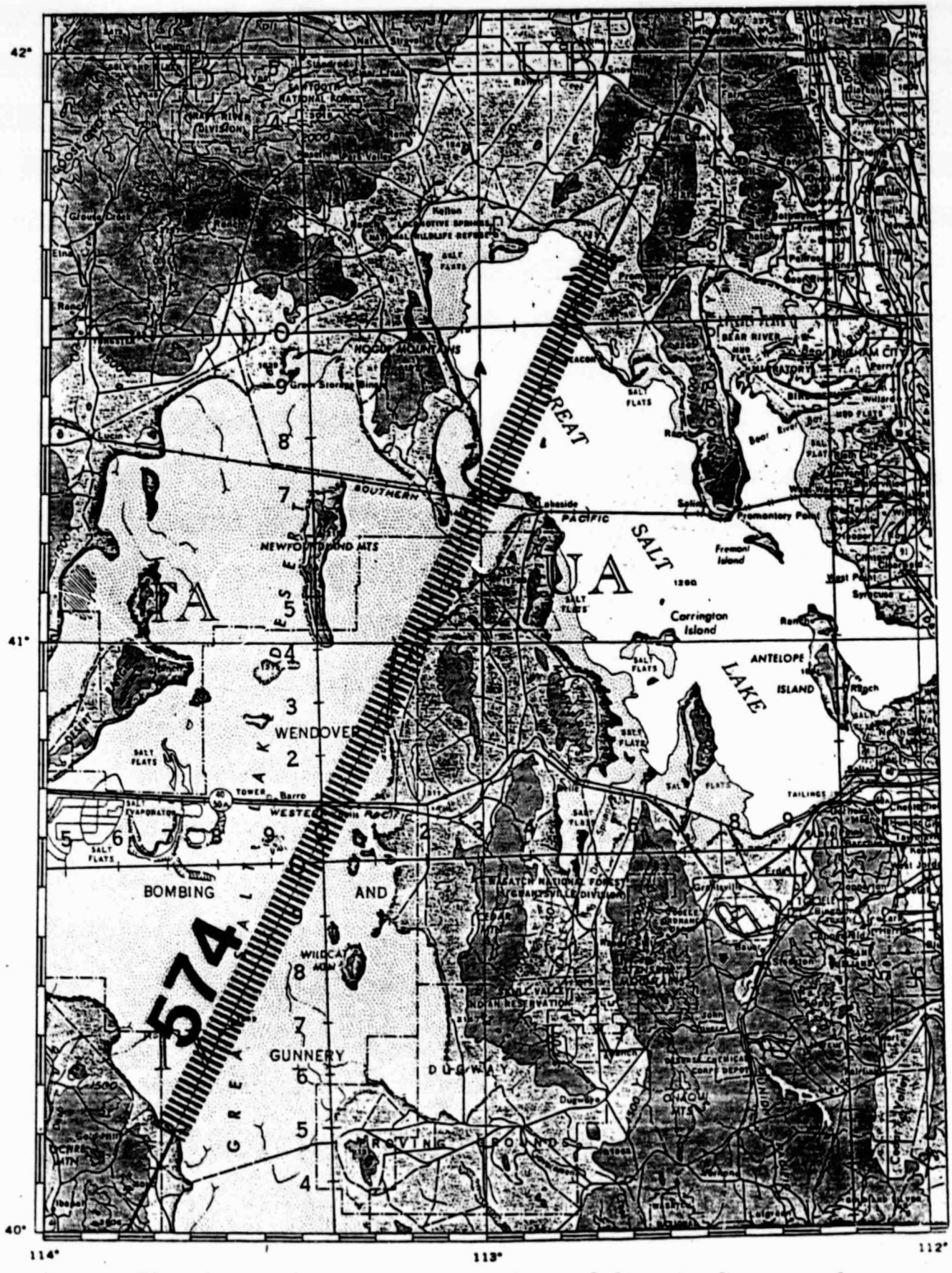

Figure 23 - Seasat Groundtrack over Great Salt Lake Desert. Cross-Hatching Indicates Period of "Lock-On".

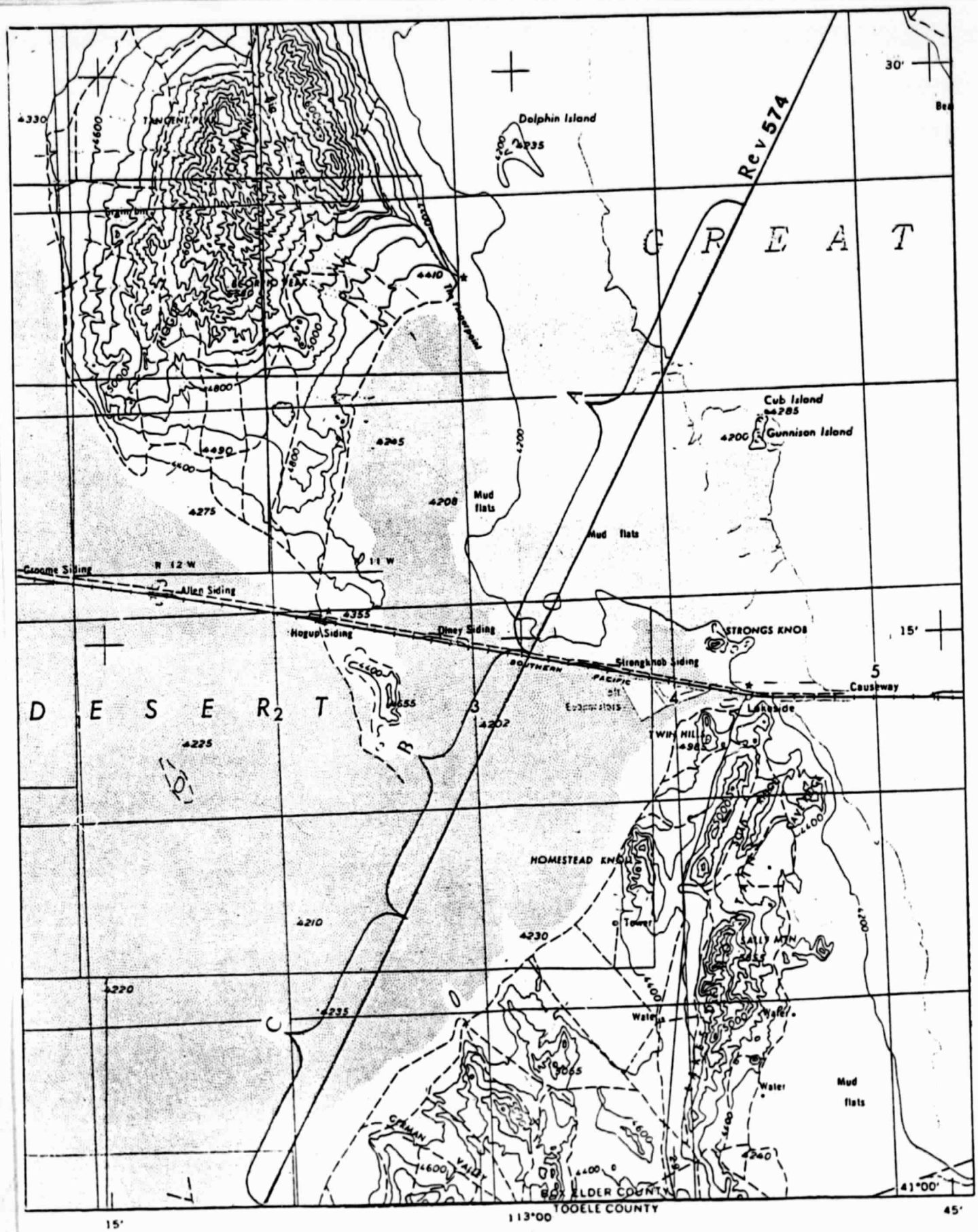

Figure 24 - Segments "A","B", and "C" of Seasat Groundtrack.

the railroad and extends southwesterly into the Great Salt Lake Desert to 41.125° latitude where the 1:24,000 map coverage ceases. Segment C continues from that point to 41.000° latitude.

The data for each of the segments is plotted in Figure 25. Segment A is at the top of the Figure. The solid line represents the terrain and lake level profile from the 1969 maps; the dots represent the altimeter-derived surface elevations. After making the altimeter and map agree at the railroad grade, the lake level at the time of the satellite flight appears to be 1.4 to 1.6 meters higher than the level shown on the 1969 maps. Investigation of the lake level fluctuations reveals that the lake elevation does change and that the position of the shoreline is extremely variable. Figure 26 is the lake-level fluctuation chart from Keck and Hassibe (1979) which also shows a comparable elevation increase since 1969.

The Dolphin Island East 1:24,000 map, dated 1969, shows a lake elevation of 4193 feet (1278 m). The Seasat altimeter indicated a lake level of 1279.4 to 1279.6 meters (4197.5 to 4198.2 feet) during this overflight with the shoreline extending to approximately 1400 meters northeast of the railroad grade.

Segment B is plotted in the middle portion of Figure 25. The correlation between the map and altimeter-derived elevations is excellent.

The bottom portion of Figure 25 illustrates Segment C altimeter elevations only as there is no 1:24,000 map covering this area. The altimeter continuously tracked across the Great Salt Lake

Figure 25 - Altimeter/Map Comparisons

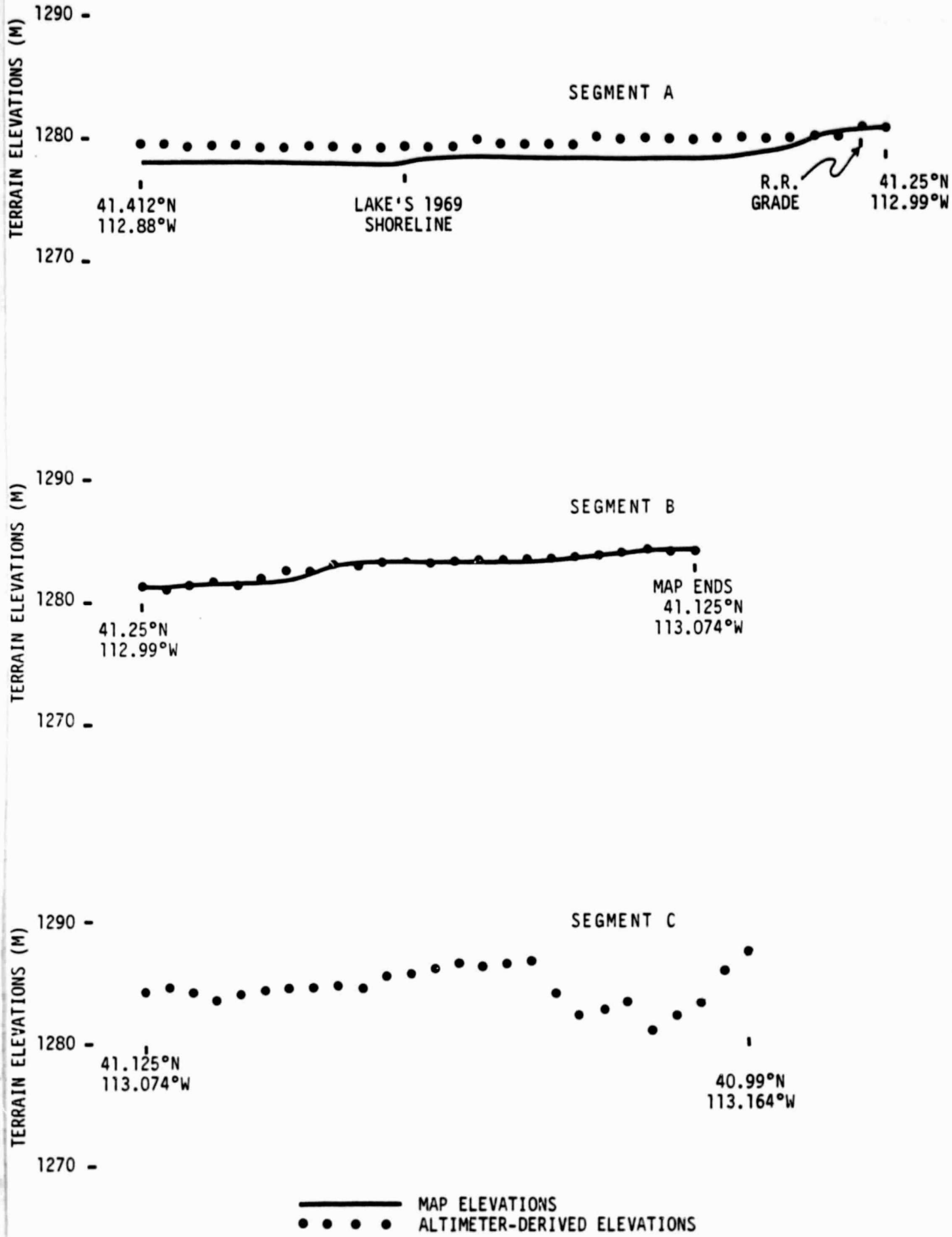

Figure 26. Great Salt Lake Level Fluctuations from Keck and Hassibe.

Desert, as shown in Figure 23, to the foothills of the Deep Creek Mountains.

The altimeter waveforms over the Great Salt Lake Desert area are plotted in Figure 27. The waveform in Figure 27A is from the Great Salt Lake and has an abrupt rise-time with a flat plateau. As the satellite neared the shoreline, the waveform was modified as shown in Figure 27B; the lake return shows up on gates 0 to +10, but after gate +10, the reflectance from the shoreline appears. The waveform for the water-to-land transition is shown in Figure 27C. The waveform over the mud flats adjacent to the lake is in Figure 27D, while a waveform over the very specular Great Salt Lake Desert appears in Figure 27E.

The USGS index to Utah topographic maps shows that a large area within the Great Salt Lake Desert is not yet covered by large scale mapping. Based on the results of this Seasat

Figure 27A - Waveform over Great Salt Lake

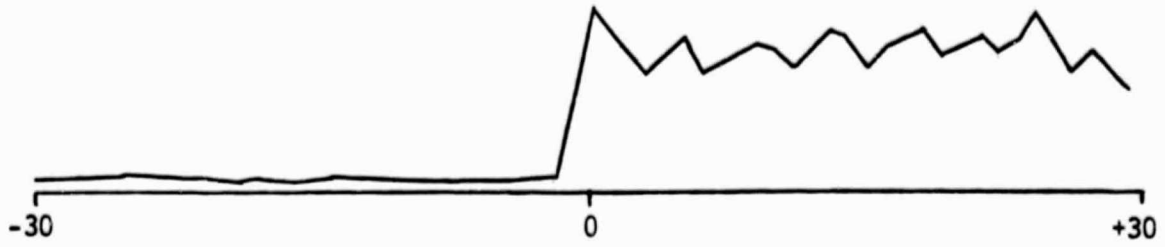

Figure 27B - Waveform over Lake with Shoreline Appearing at Gate +10

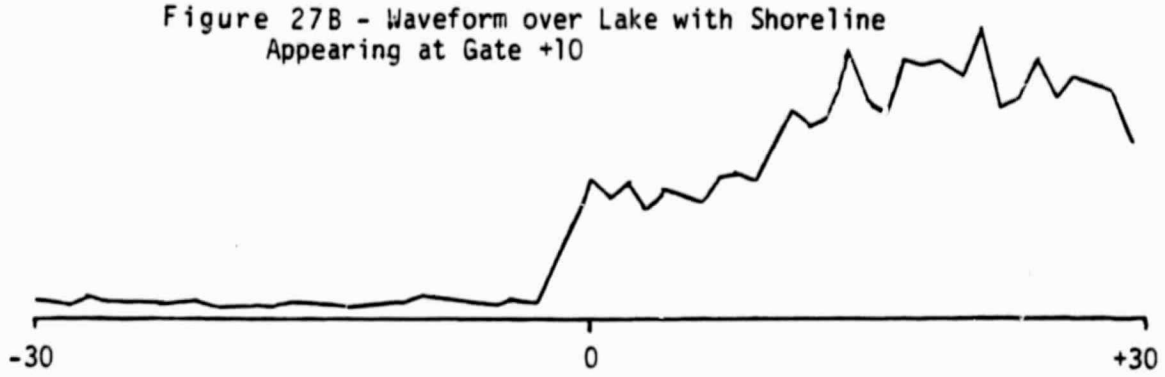

Figure 27C - Waveform at Water/Land Transition

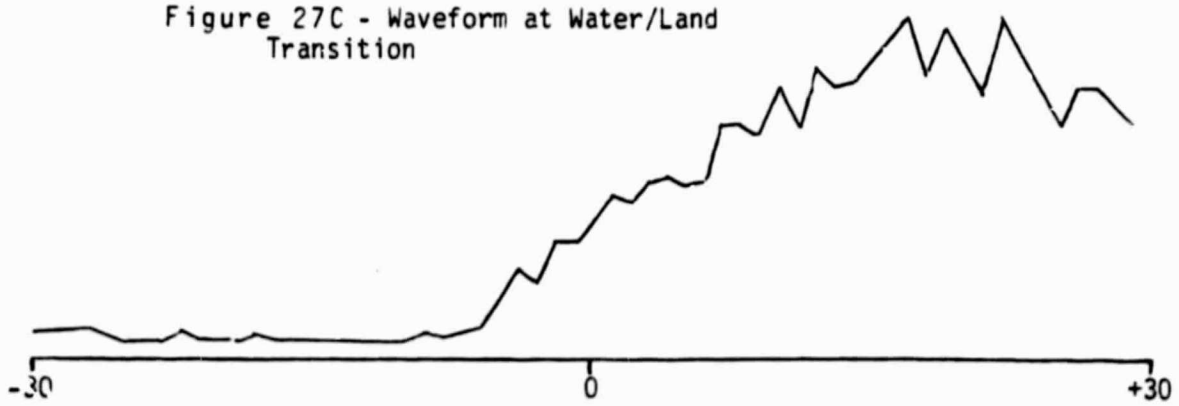

(continued on Next Page)

Figure 27D - Waveform over Mud Flats

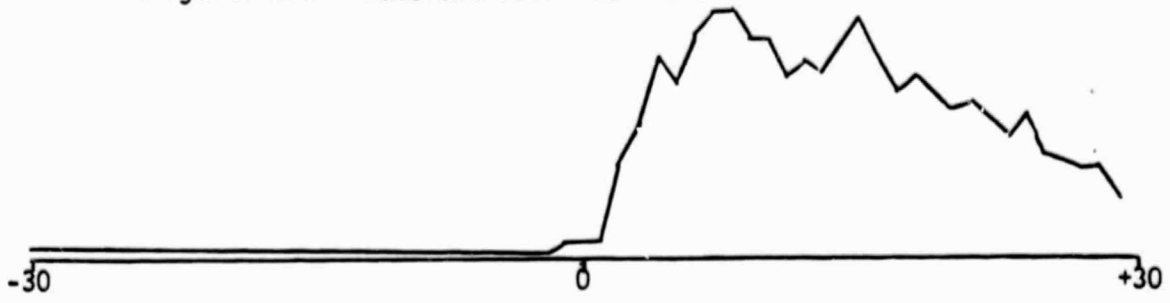

Figure 27E - Waveform over
Great Salt Lake Desert

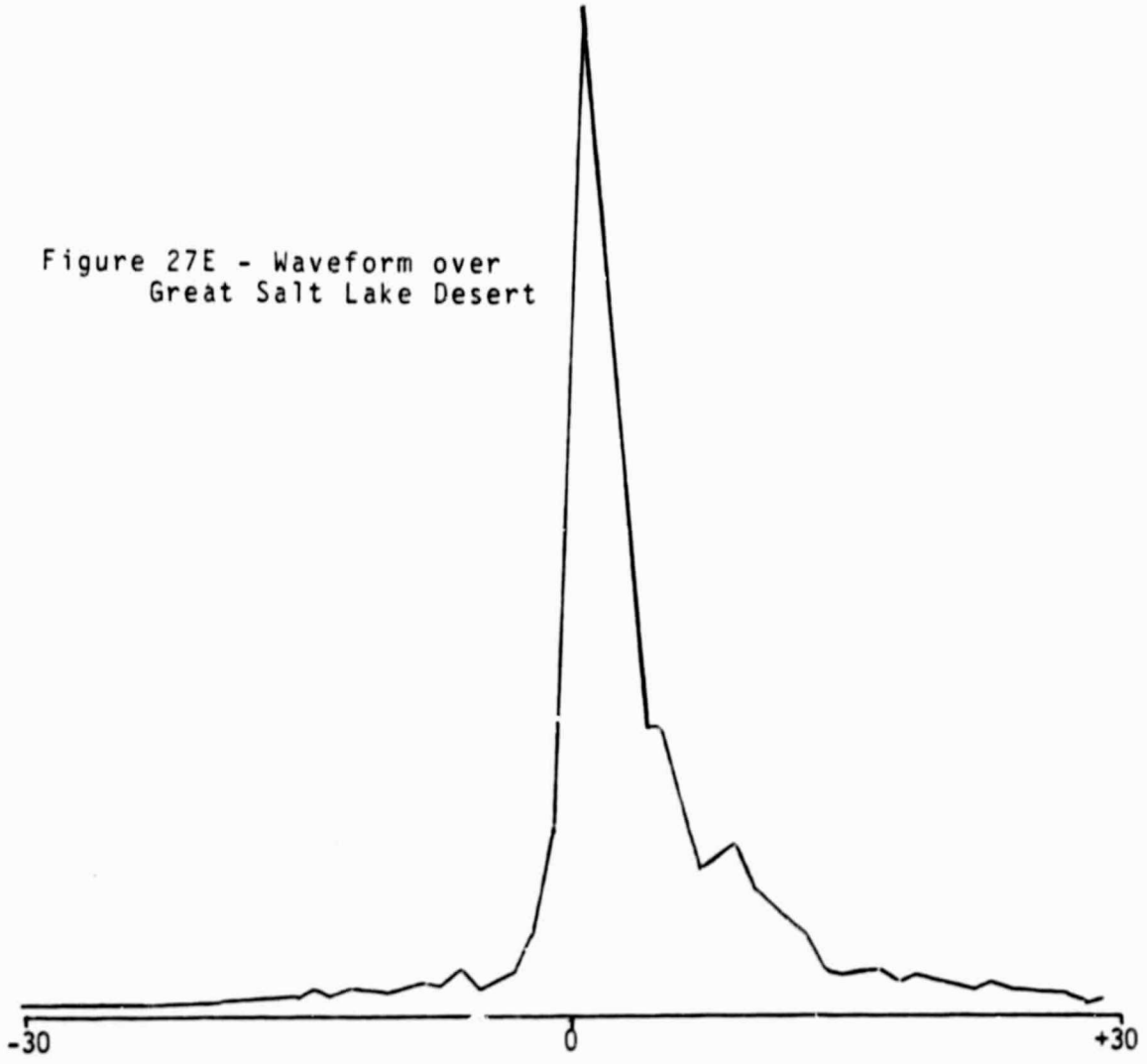

analysis over the Great Salt Lake Desert, it is concluded that existing satellite radar altimeter data (Seasat and GEOS-3) could be utilized to provide complementary vertical control for USGS mapping of this area, and thus reduce the time and costs normally required for map preparation.

SUMMARY

The Seasat altimeter did maintain lock over areas of subdued topography. The on-board tracker was not sufficiently responsive to terrain changes or terrain reflectivity, but the archived waveforms may be retracked to produce an invaluable data base for terrain mapping, regional tectonic studies, monitoring of vertical crustal movements, and ice sheet topography.

In particular, the data should be considered for the following overland applications:

1) supplementary vertical control in U. S. areas such as Alaska and the Great Salt Lake Desert, where large-scale mapping is not completed.

2) reconnaissance of areas where vertical crustal movements are suspected.

3) providing the third-dimension for Landsat imagery in developing countries.

REFERENCES

Brooks, R. L., 1981, Satellite Altimeter Measurements of Land Subsidence in South-Central Arizona. GeoScience Research Corporation Report.

Carter, W. D., W. S. Kowalik, R. Ballón, and C. Brockman, Mapping Andean Salar Deposits by Landsat Radiance Values. In Press.

Jachens, R. C., and T. L. Holzer, 1979, Geophysical Investigations of Ground Failure Related to Ground-Water Withdrawal - Picacho Basin, Arizona. In Ground Water, Vol. 16, No. 6.

Keck, W. G., and W. R. Hassibe, 1979, The Great Salt Lake. U. S. GPO 1979 0-307-854.

Laney, R. L., R. H. Raymond, and C. C. Winikka, 1978, Maps Showing Water-Level Declines, Land Subsidence, and Earth Fissures in South-Central Arizona. U.S.G.S. Water-Resources Investigations 78-83 Open File Report.

Stoertz, G. E., and W. D. Carter, 1976, Hydrogeology of Closed Basins and Deserts of South America. In ERTS-1 A New Window On Our Planet (U.S.G.S. Professional Paper 929).

Winikka, C. C., and P. D. Wold, 1976, Land Subsidence in Central Arizona. International Association of Hydrological Sciences Publication No. 121.